ELECTRONIC SUPPLEMENTARY INFORMATION

Templation effect as a driving force for self-assembly of hydrogen-bonded peptidic capsules in competitive media

M. Grajda, M. J. Lewińska and A. Szumna

Table of contents

1. General information

All solvents and chemicals used were purchased from Sigma Aldrich, TCI Europe N. V., Roth, Chem Impex Inc. and Euriso-top, were of reagent grade and were used without further purification. All reactions were carried out under atmosphere of air.

^{1}H and ^{13}C NMR spectra were recorded at 303 K on Bruker 400 MHz and at 298 K on Varian VNMRS 600 MHz instruments with a residual solvent signal as an internal standard. All 2D NMR spectra were recorded at 298 K on a Varian 600 MHz instrument with a residual solvent signal as an internal standard. The use of deuterated solvent had no influence on the properties of the investigated capsules.

High-resolution ESI mass spectra were recorded on a SYNAPT spectrometer.

Optical rotations were recorded on Jasco P-2000 polarymeter.

ECD spectra were recorded on ECD Jasco J-715 spectropolarimeter.

Mechanochemical experiments were carried out using Retsch Planetary Ball Mill PM 100.

2. Synthetic procedures for hydrazides

2.1. Hydrazide **2a**

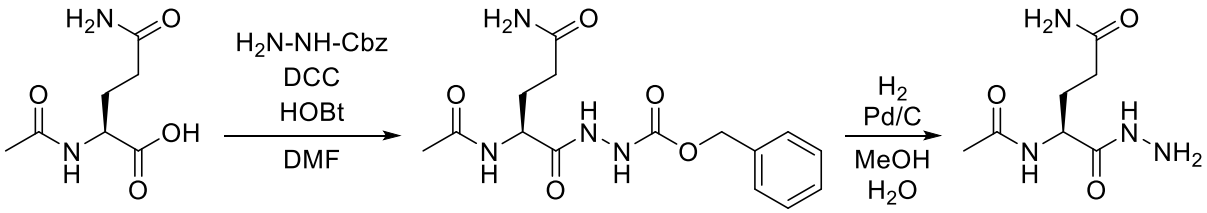

Ac-L-Gln-NH-NH-Cbz (**S2**)**:** To solution of Ac-L-Gln-OH **S1** (1.0 equiv., 7.528 g, 40.0 mmol) and carbobenzoxyhydrazide (H_2N-NH-Cbz) (1.0 equiv., 6.648 g, 40.0 mmol) in DMF (150 ml), HOBt hydrate (1.0 equiv., 6.126 g, 40.0 mmol) was added and the soloution was stirred at 0 °C for 30 min. Next, DCC (2.0 equiv., 16.504 g, 80.0 mmol) was added and the reaction mixture was stirred at 0 °C for 4 h and for additional 20 h at room temperature. The white precipitate of DCU was filtered off and the solvent was removed under reduced pressure. The residue was suspended in water (ca. 500 ml), heated to reflux and the insoluble residue was filtered off. The solvent was removed under reduced pressure and the off-white solid residue was washed with iPrOH and dried under reduced pressure, affording a white solid of Ac-L-Gln-NH-NH-Cbz **S2** (8.537 g, 64%).

Optical rotation: $[\alpha]_D$ -20.6 (c 1.01 in MeOH)

^{1}H NMR (400 MHz, DMSO-d_6) δ 9.81 (s, 1H), 9.18 (s, 1H), 8.05 (d, *J* = 8.2 Hz, 1H), 7.41 – 7.28 (m, 5H), 7.22 (s, 1H), 6.72 (s, 1H), 5.08 (s, 2H), 4.27 (td, *J* = 8.4, 5.7 Hz, 1H), 2.12 (t, *J* = 7.3 Hz, 2H), 1.94 – 1.85 (m, 1H), 1.84 (s, 3H), 1.76 – 1.65 (m, 1H).

^{13}C NMR (100 MHz, DMSO-d_6) δ 174.05, 171.75, 169.62, 156.42, 137.08, 128.83, 128.41, 128.27, 66.32, 51.08, 31.82, 28.58, 22.95.

HRMS (ESI-TOF): calcd m/z for $C_{15}H_{20}N_4O_5Na^+$ [M + Na]$^+$: 359.1331; found: 359.1330.

Ac-L-Gln-NH-NH$_2$ (2a): To a suspension of Ac-L-Gln-NH-NH-Cbz **S2** (8.412, 25.01 mmol) in MeOH:H_2O (150 ml, 1:1, v:v) at room temperature kept under argon atmosphere, palladium 10% on activated carbon was added. Hydrogen gas was purged through the solution. The reaction was monitored by TLC (MeOH:CH_2Cl_2, 1:4, v:v) with ninhydrine staining. After consumption of the substrate, the catalyst was filtered off through the Celite® and washed with water (ca. 50 ml). The solvent was evaporated under reduced pressure and the residue was washed with MeOH and dried under reduced pressure, giving Ac-L-Gln-NH-NH$_2$ **2a** (2.482 g, 97%) as a white solid.

Optical rotation: $[\alpha]_D$ -23.5 (c 1.02 in H_2O)

^{1}H NMR (400 MHz, DMSO-d_6) δ 9.08 (s, 1H), 7.96 (d, *J* = 8.2 Hz, 1H), 7.24 (s, 1H), 6.71 (s, 1H), 4.20 (bs, 2H), 4.16 (td, *J* = 8.4, 5.9 Hz, 1H), 2.11 – 1.96 (m, 2H), 1.83 (s, 3H), 1.88 – 1.76 (m, 1H), 1.73 – 1.60 (m, 1H).

^{13}C NMR (100 MHz, DMSO-d_6) δ 173.61, 170.67, 169.15, 50.97, 31.51, 28.09, 22.53.

Combustion elemental analysis: Calculated for $C_7H_{14}N_4O_3{\cdot}(CH_3OH)_n$ (n=0.2, MeOH also observed in ^{1}H NMR spectrum): C, 41.45; H, 7.15; N, 26.86. Found: C, 41.63; H, 7.02; N, 26.53.

HRMS (ESI-TOF): calcd m/z for $C_7H_{14}N_4O_3Na^+$ [M + Na]$^+$: 225.0963; found: 225.0964.

2.2. Hydrazide **2b**

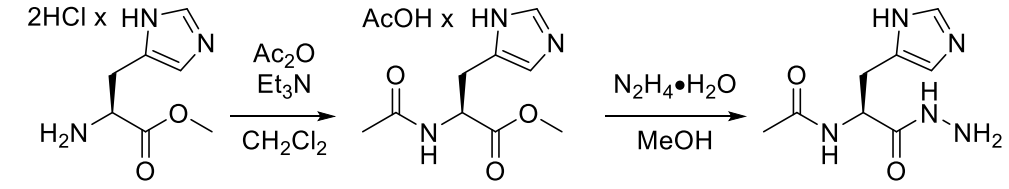

H-L-His-OMe x 2HCl **S3** | Ac-L-His-OMe x AcOH **S4** | Ac-L-His-NH-NH2 **2b**

Ac-L-His-OMe·AcOH (**S4**): To a suspension of H-L-His-OMe x 2 HCl **S3** (1.2 g, 4.96 mmol) in DCM (200 ml) Et_3N (2 equiv., 1.4 ml, 10.0 mmol) was added. Then Ac_2O (4.6, 2.17 ml, 23 mmol) was added dropwise and the reaction was stirred at room temperature for 20 h. The mixture was washed with saturated aqueous solution of Na_2CO_3 (2 x 50 ml). The organic layer was collected and the solvent was evaporated under reduced pressure. The residue was dried under reduced pressure, giving of Ac-L-His-OMe·AcOH **S4** (0.902 g, 67%) as a white solid.

^{1}H NMR (400 MHz, DMSO-d_6) δ 8.31 (d, J = 1.2 Hz, 1H), 8.22 (d, J = 7.6 Hz, 1H), 7.42 (d, J = 1.1 Hz, 1H), 4.51 (td, J = 8.4, 5.5 Hz, 1H), 3.61 (s, 3H), 2.91 (dd, J = 15.0, 5.3 Hz, 1H), 2.82 (dd, J = 14.8, 8.6 Hz, 1H), 2.58 (s, 3H), 1.81 (s, 3H).

^{13}C NMR (100 MHz, DMSO-d_6) δ 172.03, 169.36, 167.52, 139.15, 137.28, 113.36, 51.81, 51.68, 29.65, 22.57, 22.26.

Ac-L-His-NH-NH$_2$ (**2b**): To a solution of Ac-L-His-OMe x AcOH **S4** (1.27 g, 4.68 mmol) in MeOH (50 ml) hydrazine monohydrate(3 equiv., 0.68 ml, 14.0 mmol) was added and the reaction was stirred for 24 h at room temperature. During the reaction a white precipitate was formed. The precipitate, being the first fraction of product **2b**, was filtered off. The filtrate was evaporated under reduced pressure to dryness. The off-white solid residue was washed with $CHCl_3$ (10 ml), resulting in the second fraction of **2a** as a white solid. Both solids were dried under reduced pressure. The collective yield of Ac-L-His-NH-NH$_2$ **2b** is 97% (0.959 g). It is important to note that the purity of the second fraction was worse than the first fraction.

Optical rotation: $[\alpha]_D$ -10.0 (c 1.00 in H_2O)

^{1}H NMR (400 MHz, DMSO-d_6) δ 11.72 (bs, 1H), 9.09 (s, 1H), 7.99 (d, *J* = 8.2 Hz, 1H), 7.49 (d, *J* = 1.0 Hz, 1H), 6.74 (s, 1H), 4.42 (ddd, *J* = 8.3, 5.8 Hz, 1H), 4.18 (bs, 2H), 2.87 (dd, *J* = 14.7, 5.7 Hz, 1H), 2.72 (dd, *J* = 14.8, 8.4 Hz, 1H), 1.80 (s, 3H).

^{13}C NMR (100 MHz, DMSO-d_6) δ 170.45, 169.02, 134.54, 133.31, 117.00, 51.44, 29.86, 22.62.

Combustion elemental analysis: Calculated for $C_8H_{13}N_5O_2$: C, 45.49; H, 6.20; N, 33.16. Found: C, 45.43; H, 6.25; N, 32.84.

HRMS (ESI-TOF): calcd m/z for $C_8H_{13}N_5O_2Na^+$ $[M + Na]^+$: 234.0967; found: 234.0957.

3. Experimental procedures for cavitands

3.1. Cavitand **3a**

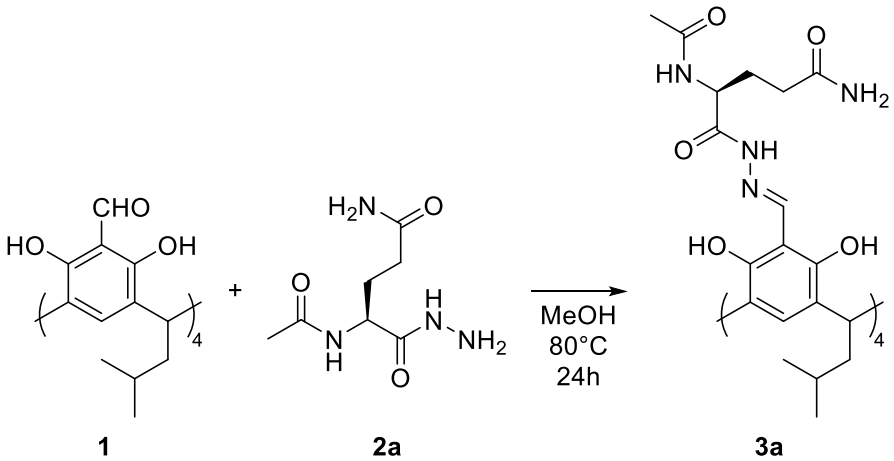

1 **2a** **3a**

Cavitand **3a:** Tetraformylresorcin[4]arene **1** (1.0 equiv., 176 mg, 0.187 mmol) and Ac-L-Gln-NH-NH$_2$ **2a** (4.5 equiv., 170 mg, 0.841 mmol) were suspended in MeOH (15 ml) in a screw-capped vial and stirred at 80 °C for 24 h. The solvent was evaporated under reduced pressure and the crude residue was washed with water (ca. 15 ml) and dried under reduced pressure giving cavitand **3a** (254 mg, 87%) as an orange solid.

Optical rotation: $[\alpha]_D$ -14.3 (c 1.03 in DMSO)

^{1}H NMR (600 MHz, DMSO-d_6) δ 11.75 (s, 1H), 10.84 (s, 1H), 8.72 (s, 1H), 8.20 (d, *J* = 7.2 Hz, 1H), 7.48 (s, 1H), 7.28 (s, 1H), 6.75 (s, 1H), 4.56 (t, *J* = 6.5 Hz, 1H), 4.20 (dd, *J* = 14.1, 7.3 Hz, 1H), 2.13 – 2.08 (m, 1H), 2.09 – 2.05 (m, 1H), 1.94 – 1.87 (m, 1H), 1.86 (s, 3H), 1.82 – 1.73 (m, 1H), 1.42 – 1.34 (m, 1H), 0.94 (dd, *J* = 9.0, 3.0 Hz, 6H).

^{13}C NMR (150 MHz, DMSO-d_6) δ 173.33, 169.52, 167.75, 151.94, 146.61, 128.10, 123.67, 106.40, 51.53, 42.28, 31.25, 30.63, 27.40, 25.97, 22.77, 22.69, 22.46.

HRMS (ESI-TOF): calcd m/z for $C_{76}H_{103}N_{16}O_{20}^-$ [M - H]$^-$: 1559.7535; found: 1559.7538.

3.2. Cavitand **3b**

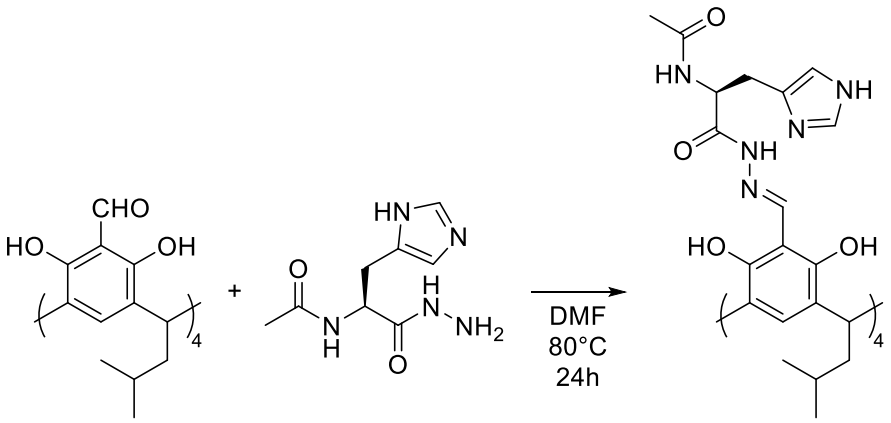

1 **2b** **3b**

Cavitand **3b:** Tetraformylresorcin[4]arene **1** (1.0 equiv., 141.3 mg, 0.150 mmol) and Ac-L-His-NH-NH_2 **2b** (4.5 equiv., 142.5 mg, 0.675 mmol) were dissolved in DMF (15 ml) in a screw-capped vial and stirred at 80 °C for 24 h. The solvent was evaporated under reduced pressure and the crude residue was washed with water (3 x 20 ml). The precipitate was dried under reduced pressure, giving **3b** (0.148 mg, 62%) as an orange solid.

Optical rotation: $[\alpha]_D$ -34.7 (c 0.25 in DMF)

^{1}H NMR (600 MHz, DMSO-d_6) δ 11.62 (s, *J* = 63.6 Hz, 1H), 8.71 (s, 1H), 8.22 (d, *J* = 7.7 Hz, 1H), 7.76 (s, 1H), 7.38 (s, 1H), 6.89 (s, 1H), 4.55 (t, 1H), 4.49 (dd, *J* = 14.5, 7.5 Hz, 1H), 2.97 (dd, *J* = 14.7, 6.2 Hz, 1H), 2.83 (dd, *J* = 14.7, 7.9 Hz, 1H), 2.03 (s, 2H), 1.84 (s, 1H), 1.42 – 1.33 (m, 1H), 0.93 (dd, *J* = 6.2, 2.0 Hz, 6H).

^{13}C NMR (150 MHz, DMSO-d_6) δ 169.35, 167.02, 153.56, 147.72, 134.55, 132.60, 127.63, 123.08, 116.65, 106.07, 51.89, 42.16, 29.19, 25.93, 22.82, 22.76, 22.55.

HRMS (ESI-TOF): calcd m/z for $C_{80}H_{99}N_{20}O_{16}^-$ [M - H]$^-$: 1595.7548; found: 1595.7521.

4. C_{60} complexation experiments

4.1. $(3a)_2 \supset C_{60}$ complex

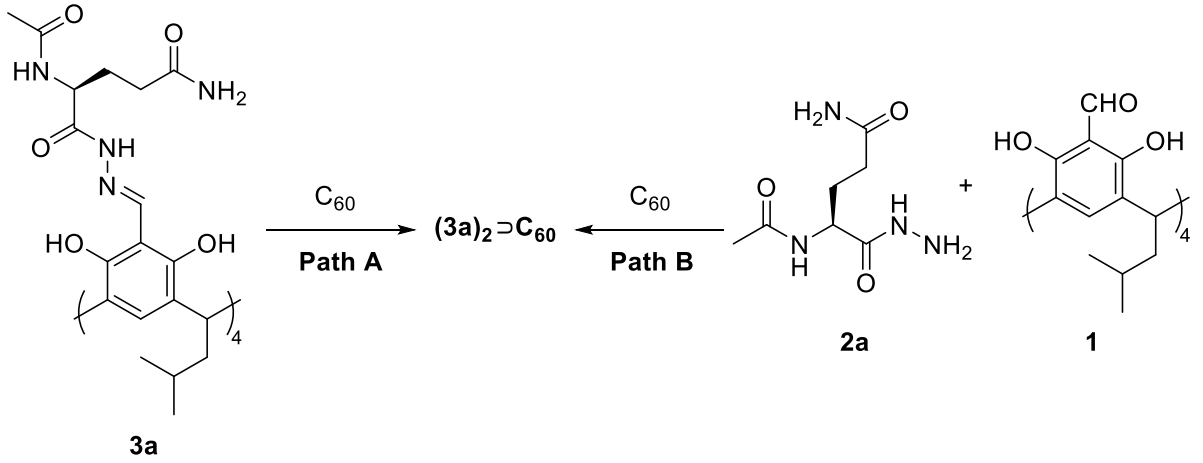

General procedures for optimization of $(3a)_2 \supset C_{60}$ formation:

Path A: Cavitand **3a** (15.6 mg, 0.01 mmol) and C_{60} (3.6 mg, 0.005 mmol) were suspended in DMSO-d_6 (0.8 ml) in a screw capped vial and stirred at 80 °C for 24 h. The residue (uncomplexed fullerene) was removed by centrifugation. The mixtures contained only two types of species: $(3a)_2 \supset C_{60}$ and **3a**. Yields of complexation were determined by NMR.

Path A*: Cavitand **3a** (15.6 mg, 0.01 mmol) and C_{60} (3.6 mg, 0.005 mmol) were milled in a planetary ball-mill for 2h (500 rpm) without solvent. The resulting solid was suspended in DMSO-d_6 (0.8 ml) and the undissolved residue (uncomplexed fullerene) was removed by centrifugation. The residue (uncomplexed fullerene) was removed by centrifugation. The mixtures contained only two types of species: $(3a)_2 \supset C_{60}$ and **3a**. Yields of complexation were determined by NMR.

Path B: Tetraformylresorcin[4]arene **1** (9.4 mg, 0.01 mmol), hydrazide **2a** (8.1 mg, 0.04 mmol) and C_{60} (3.6 mg, 0.005 mmol) were suspended in DMSO-d_6 (0.8 ml) in a screw capped vial and stirred at 80 °C for 24 h. The residue (uncomplexed fullerene) was removed by centrifugation. The mixtures contained only two types of species: $(3a)_2 \supset C_{60}$ and **3a**. Yields of complexation were determined by NMR.

Path B*: Tetraformylresorcin[4]arene **1** (9.4 mg, 0.01 mmol), hydrazide **2a** (8.1 mg, 0.04 mmol) and C_{60} (3.6 mg, 0.005 mmol) were milled in a planetary ball-mill for 2h (500 rpm) without solvent. The resulting solid was suspended in DMSO-d_6 (0.8 ml) and the undissolved residue (uncomplexed fullerene) was removed by centrifugation. The residue (uncomplexed fullerene) was removed by centrifugation. The mixtures contained only two types of species: $(3a)_2 \supset C_{60}$ and **3a**. Yields of complexation were determined by NMR.

The highest-yielding procedure for synthesis of $(3a)_2 \supset C_{60}$: Tetraformylresorcin[4]arene **1** (94.2 mg, 0.1 mmol), hydrazide **2a** (80.8 mg, 0.4 mmol) and C_{60} (72.1 mg, 0.1 mmol) were milled in a planetary ball-mill for 2h (500 rpm) without solvent. The resulting brown solid was suspended in MeOH (2ml) and the undissolved residue was removed by centrifugation. The supernatant was placed into vial and left over for two days. During that time dark brown/red regular shaped crystals were formed. The solvent was decanted and crystals

were dried under reduced pressure. The crystals obtained this way contain (**3a**)$_2$⊃C_{60} (60%) and cavitand **3a** (40%).

^{1}H NMR (600 MHz, DMSO-d_6)

3a δ 11.77 (s, 1H), 10.84 (s, 2H), 8.70 (s, 1H), 8.19 (d, *J* = 7.0 Hz, 1H), 7.52 (bs, 1H), 7.27 (s, 1H), 6.74 (s, 1H), 4.55 (t, *J* = 6.3 Hz, 1H), 4.20 (dd, *J* = 14.4, 7.2 Hz, 1H), 2.09 (dd, *J* = 15.1, 7.3 Hz, 2H), 2.11 – 2.06 (m, 2H), 1.91 – 1.87 (m, 1H), 1.86 (s, 3H), 1.81 – 1.73 (m, 1H), 1.42 – 1.34 (m, 1H), 0.94 (dd, *J* = 6.6, 2.8 Hz, 6H).

(**3a**)$_2$⊃C_{60} δ 13.75 (s, 1H), 11.79 (s, 1H), 8.95 (s, 1H), 8.91 (s, 1H), 8.51 (d, *J* = 8.5 Hz, 1H), 7.65 (s, 1H), 7.39 (s, 1H), 6.81 (s, 1H), 4.66 (dd, *J* = 15.3, 7.7 Hz, 1H), 4.39 (t, *J* = 7.5 Hz, 1H), 2.31 – 2.24 (m, 1H), 2.19 (dd, *J* = 14.7, 6.7 Hz, 2H), 2.14 (s, 3H), 2.16 – 2.11 (m, 1H), 2.01 – 1.94 (m, 1H), 1.95 – 1.91 (m, 1H), 1.45 – 1.37 (m, 1H), 0.95 (dd, *J* = 6.6, 2.7 Hz, 6H).

^{13}C NMR (150 MHz, DMSO-d_6)

3a δ 173.31, 169.48, 167.73, 151.98, 146.55, 128.13, 123.72, 106.42, 51.52, 42.26, 31.27, 30.58, 27.44, 25.97, 22.75, 22.69, 22.45.

(**3a**)$_2$⊃C_{60} δ 173.45, 171.38, 165.82, 151.36, 151.20, 147.36, 141.01, 127.64, 124.43, 123.96, 106.10, 50.66, 40.77, 31.24, 30.45, 29.71, 26.09, 23.06, 22.65, 22.48.

HRMS (ESI-TOF): calcd m/z for $C_{212}H_{208}N_{32}O_{40}Na_2^{2+}$ [M + 2Na]$^{2+}$: 1943.7510; found: 1943.7505. **NOTE**: Low resolution mass spectrum indicates absence of ions for fullerene-free dimeric species (**3a**)$_2$, what proves that fullerene template is essential for diameric capsule formation (see Fig. S53).

4.2. (3b)$_2$⊃C_{60} complex

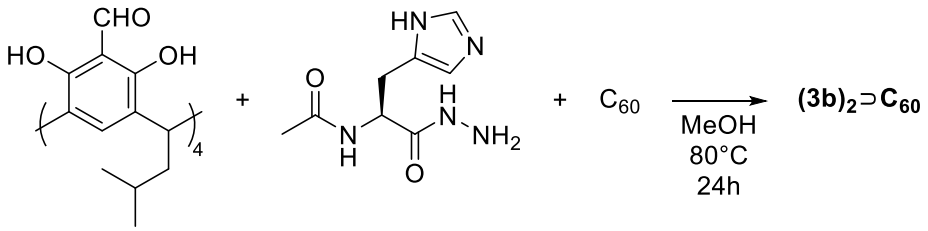

1 **2b**

(**3b**)$_2$⊃C_{60} complex: A mixture of tetraformylresorcin[4]arene **1** (1.0 equiv., 70.65 mg, 0.075 mmol), Ac-L-His-NH-NH$_2$ **2b** (4.5 equiv., 71.24 mg, 0.337 mmol) and fullerene C_{60} (1.0 equiv., 54 mg, 0.075 mmol) was suspended in MeOH (10 ml) in screw capped vial and stirred at 80 °C for 24 h. The precipitate was filtered off and the filtrate was evaporated. The residue was washed with water (3x20 ml). The precipitate was dried under reduced pressure, resulting in brown solid of (**3b**)$_2$⊃C_{60} (0.144 mg, 87%).

Optical rotation: $[\alpha]_D$ -212.0 (c 0.1 in MeOH)

^{1}H NMR (600 MHz, CD_3OD-MeOH (1:9)) δ 8.84 (s, 1H), 8.23 (d, *J* = 9.6 Hz, 1H), 7.70 (s, 1H), 7.31 (s, 1H), 6.86 (s, 1H), 5.01 (dd, *J* = 16.4, 7.3 Hz, 1H), 4.44 (t, *J* = 7.8 Hz, 1H), 3.14 (dd, *J* = 14.0, 7.1 Hz, 1H), 3.00 (dd, *J* = 14.1, 7.9 Hz, 1H), 2.12 (s, 3H), 2.10 – 2.08 (m, 1H), 2.05 – 1.98 (m, 1H), 1.42 (tt, *J* = 13.4, 6.6 Hz, 1H), 0.93 (d, *J* = 6.6 Hz, 6H).

^{13}C NMR (150 MHz, CD_3OD-MeOH (1:9)) δ 171.75, 166.99, 152.51, 152.43, 149.39, 141.96, 135.73, 131.75, 126.91, 124.66, 124.22, 119.30, 106.94, 52.38, 41.76, 31.73, 30.65, 26.33, 23.08, 22.09, 21.93.

^{1}H NMR (600 MHz, DMSO-d_6)

3b δ 11.51 (bs, 1H), 8.71 (s, 1H), 8.19 (d, J = 7.8 Hz, 1H), 7.60 (s, 1H), 7.34 (s, 1H), 6.81 (s, 1H), 4.55 (t, J = 7.6 Hz, 1H), 4.48 (dd, J = 14.4, 7.5 Hz, 1H), 22.95 (dd, J = 14.3, 5.8 Hz, 1H), 2.85 – 2.77 (m, 1H), 2.06 – 1.99 (m, 1H), 1.83 (s, 3H), 1.42 – 1.34 (m, 1H), 0.93 (d, J = 6.3 Hz, 6H).

(**3b**)$_2$⊃C_{60} δ 13.61 (s, 1H), 8.85 (s, 1H), 8.75 (s, 1H), 8.58 (d, J = 8.9 Hz, 1H), 7.86 (s, 1H), 7.61 (s, 1H), 6.90 (s, 1H), 4.85 (dd, J = 16.2, 7.9 Hz, 1H), 4.34 (t, J = 7.3 Hz, 1H), 3.09 (dd, J = 12.8, 8.3 Hz, 1H), .95 (dd, J = 14.3, 5.8 Hz, 1H), 2.21 – 2.13 (m, J = 4.8 Hz, 2H), 2.03 (s, 3H), 1.42 – 1.34 (m, 1H), 0.94 (d, J = 6.2 Hz, 6H).

^{13}C NMR (150 MHz, DMSO-d_6)

3b δ 169.27, 167.03, 153.91, 148.13, 134.60, 127.66, 116.70, 105.97, 51.98, 42.13, 30.36, 29.53, 25.91, 22.83, 22.77, 22.56.

(**3b**)$_2$⊃C_{60} δ 170.86, 165.29, 151.21, 151.12, 147.43, 140.90, 135.48, 124.28, 123.98, 105.94, 51.84, 40.74, 31.58, 30.36, 26.05, 22.96, 22.54, 22.49.

HRMS (ESI-TOF): calcd m/z for $C_{220}H_{204}N_{40}O_{32}^{4+}$ $[M + 4H]^{-}$: 3917.55434; found: 3917.54240. **NOTE**: The low resolution mass spectrum indicates absence of ions for fullerene-free dimeric species (**3b**)$_2$, what proves that fullerene template is essential for dimeric capsule formation (see Fig. S54).

5. Spectra

5.1. NMR Spectra

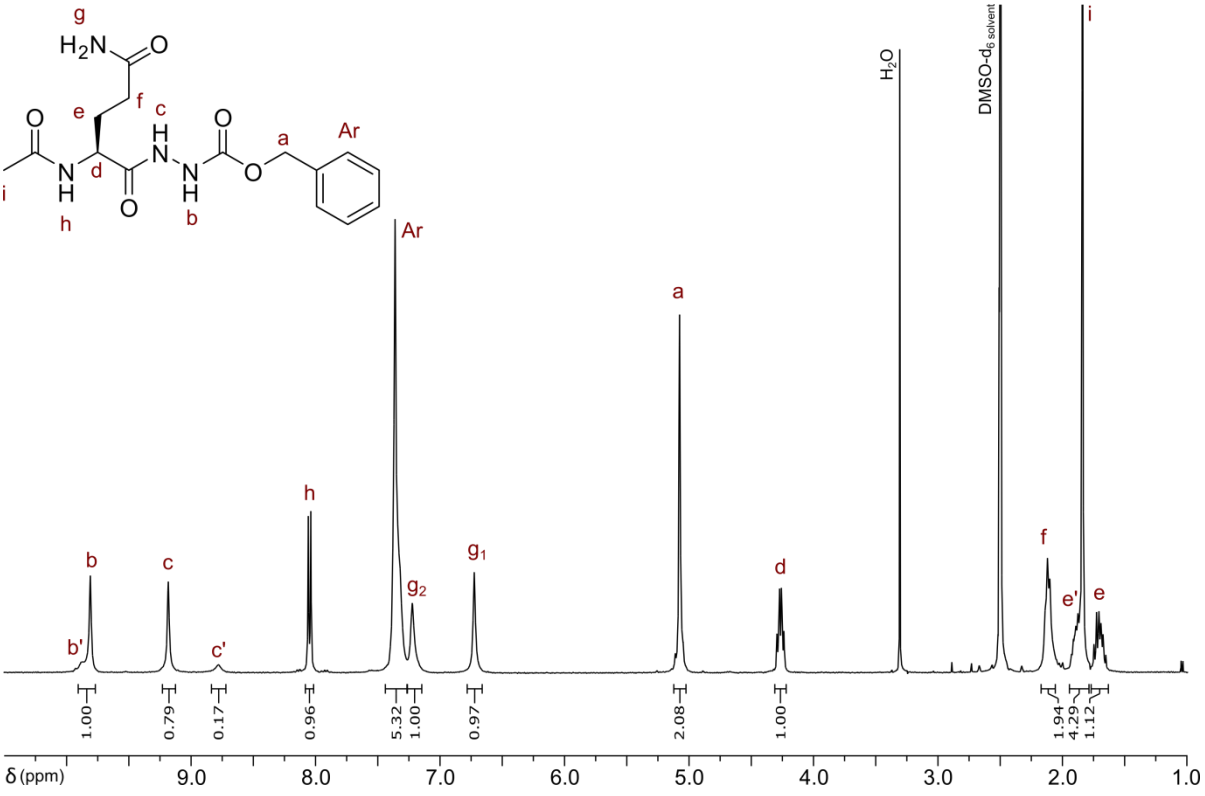

Fig. S1. ^{1}H NMR spectrum of **S2** (400 MHz, DMSO-d_6).

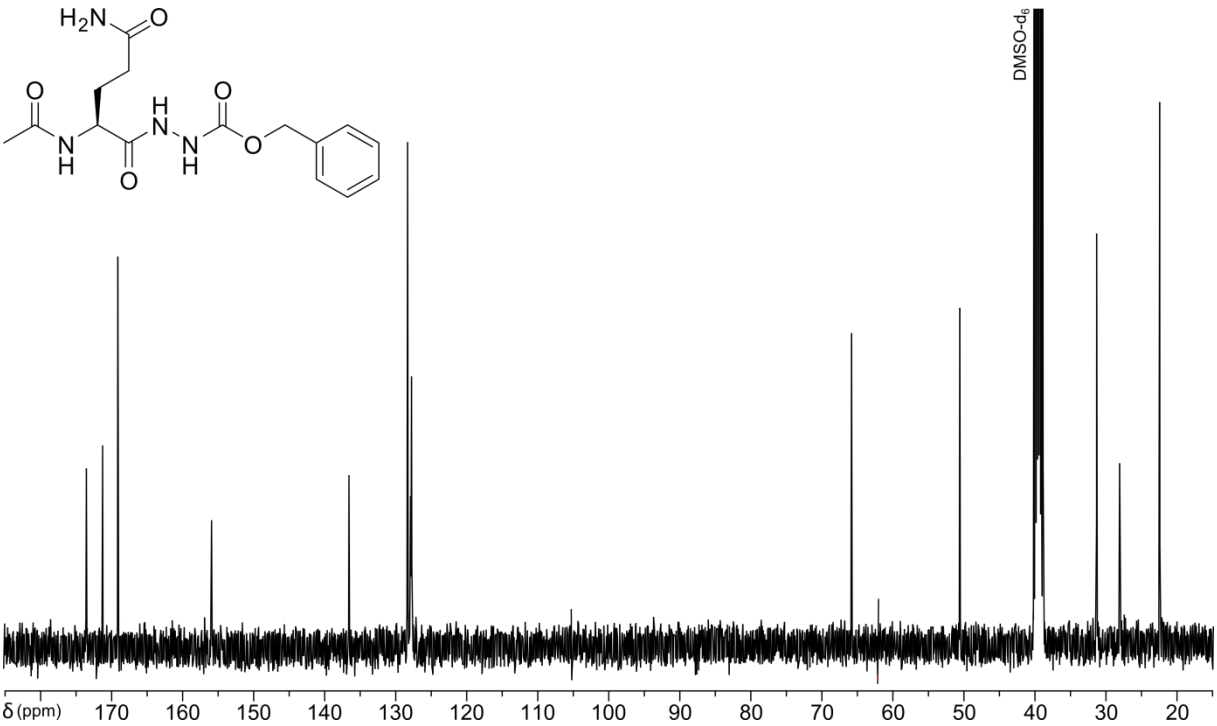

Fig. S2. ^{13}C NMR spectrum of **S2** (100 MHz, DMSO-d_6).

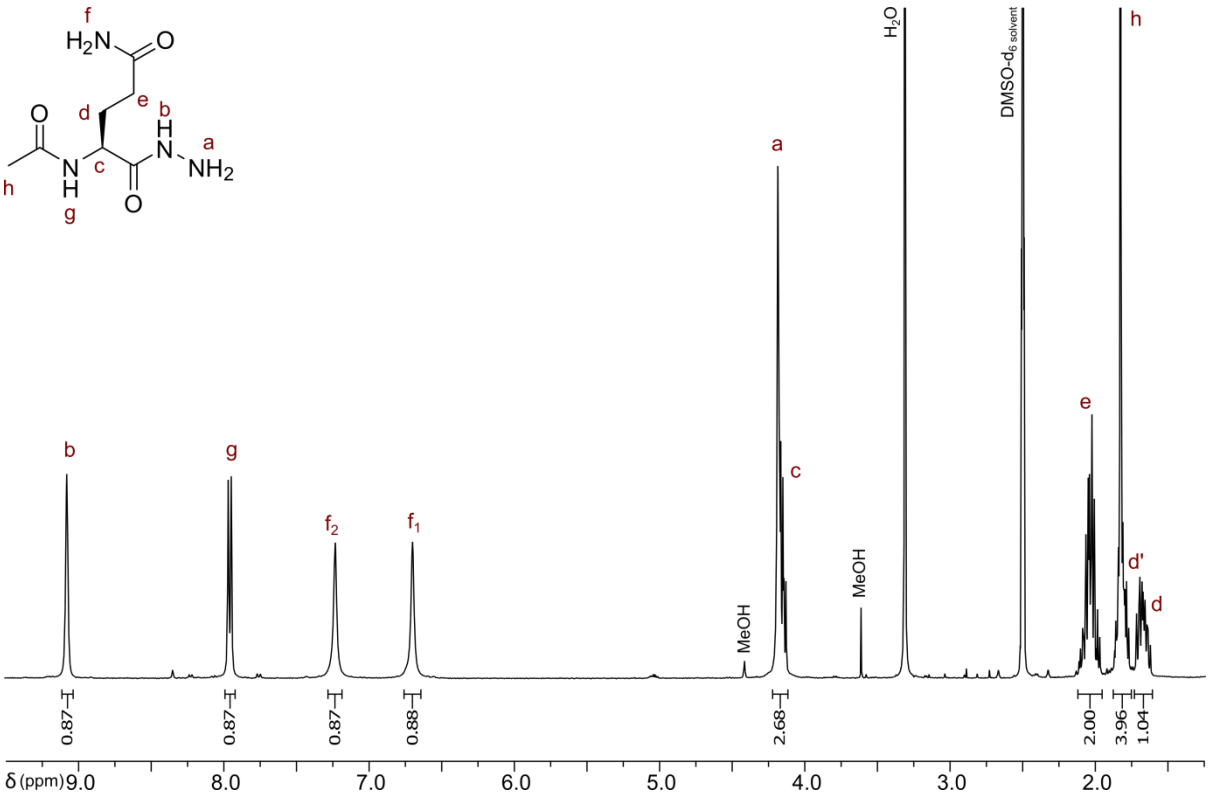

Fig. S3. ^{1}H NMR spectrum of **2a** (400 MHz, DMSO-d_6).

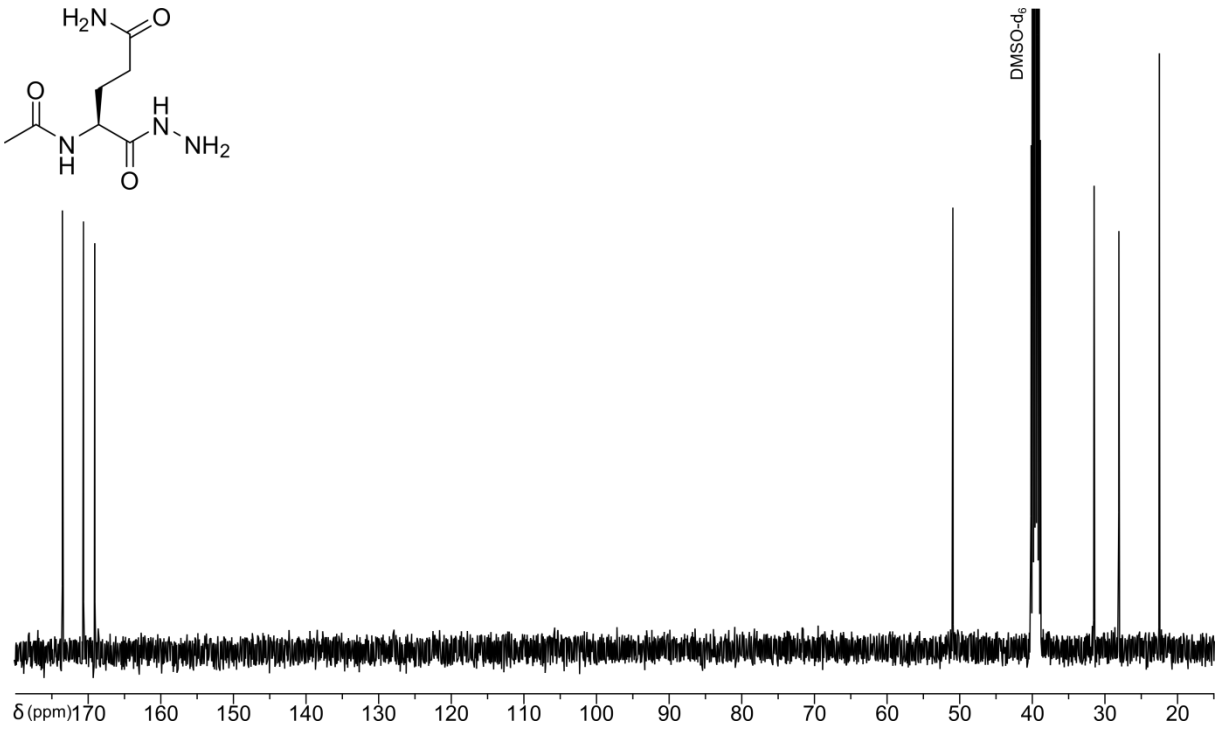

Fig. S4. ^{13}C NMR spectrum of **2a** (100 MHz, DMSO-d_6).

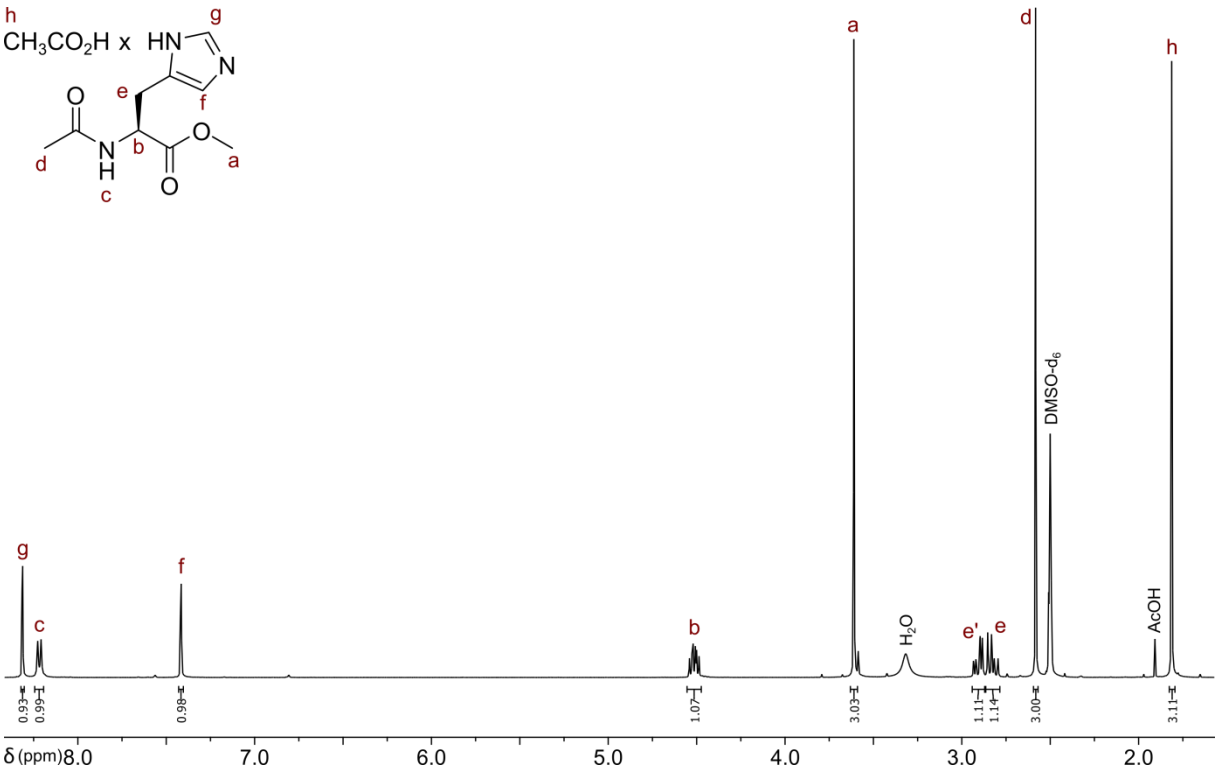

Fig. S5. ^{1}H NMR spectrum of **S4** (400 MHz, DMSO-d_6).

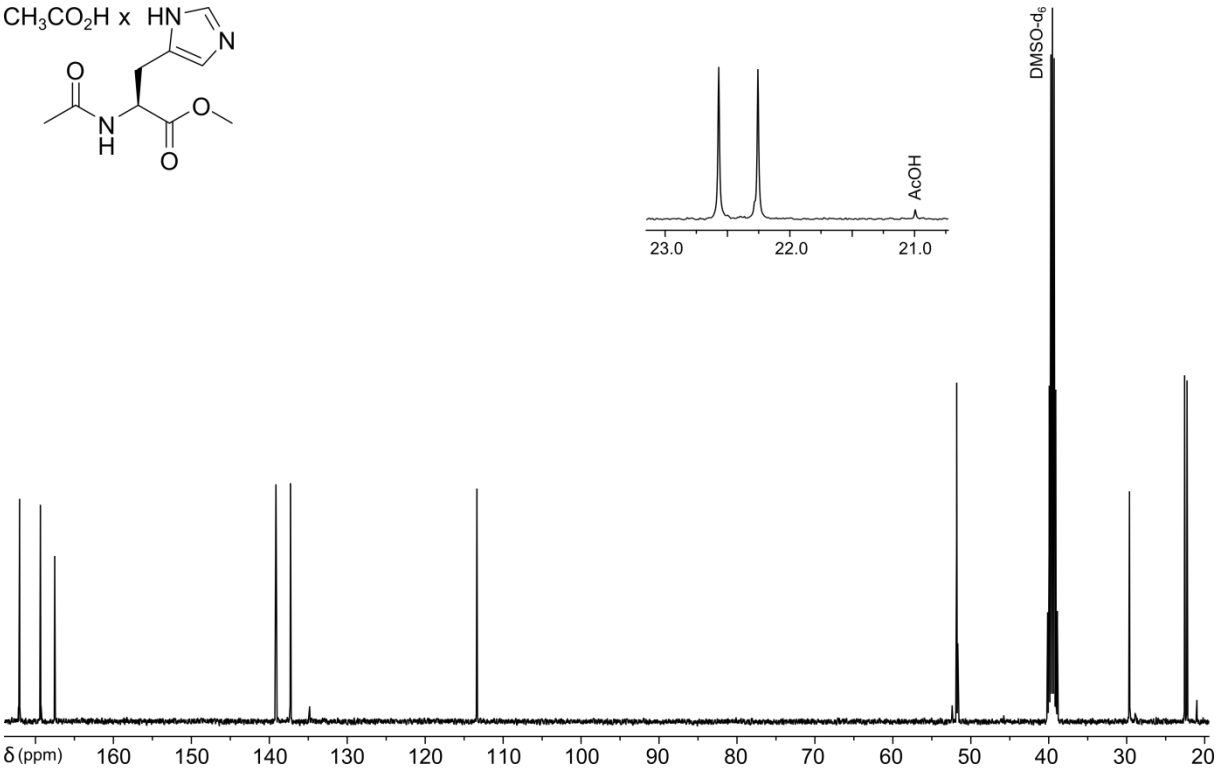

Fig. S6. ^{13}C NMR spectrum of **S4** (100 MHz, DMSO-d_6).

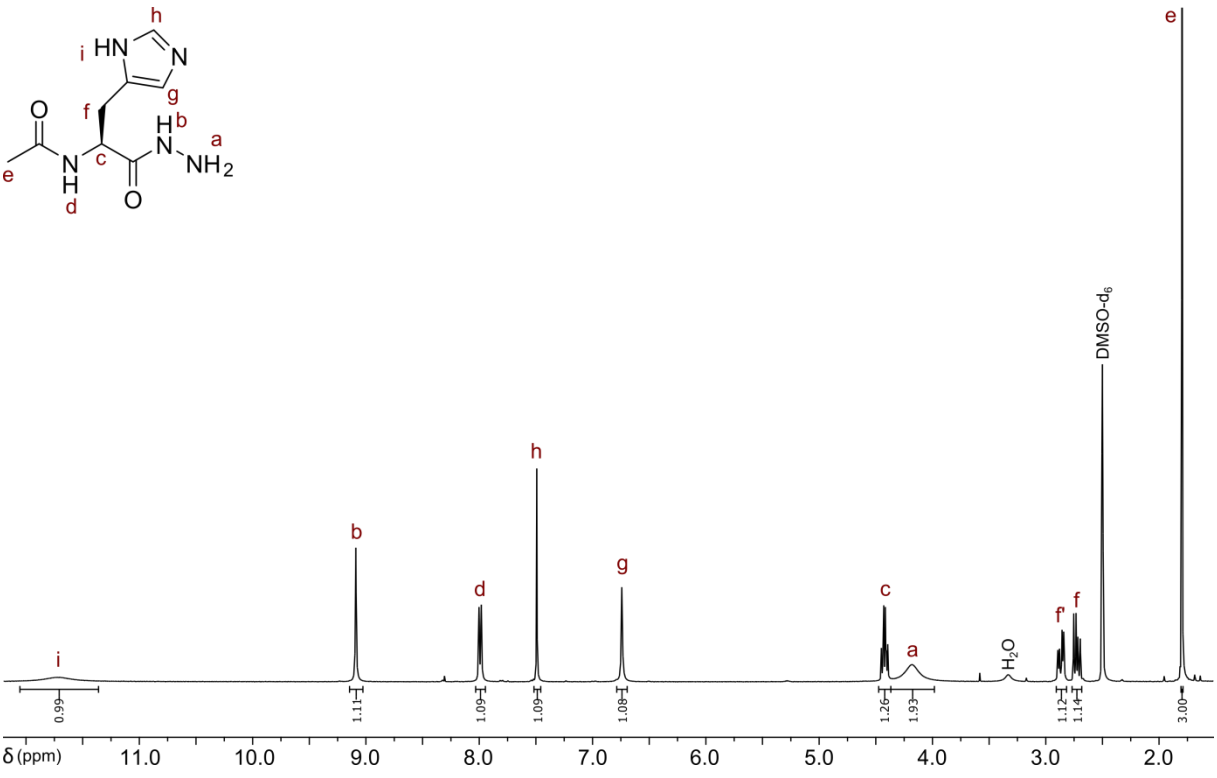

Fig. S7. ^{1}H NMR spectrum of **2b** (400 MHz, DMSO-d_6).

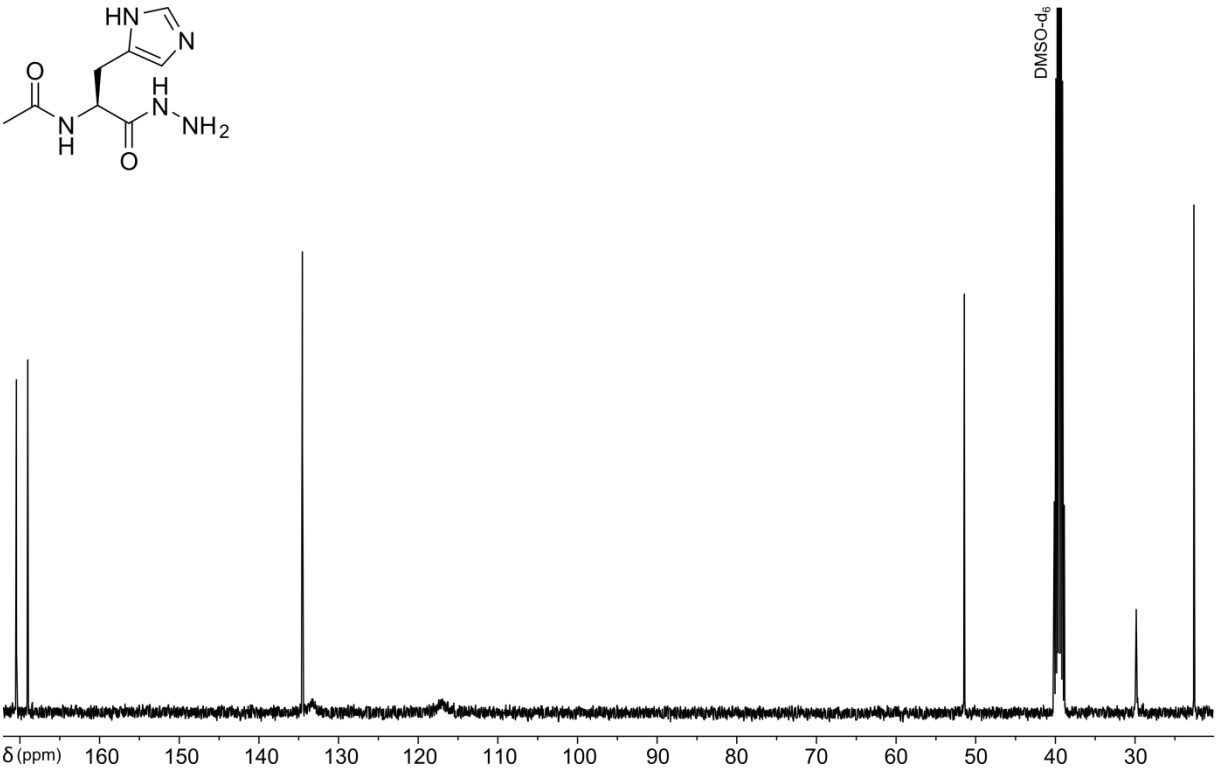

Fig. S8. ^{13}C NMR spectrum of **2b** (100 MHz, DMSO-d_6).

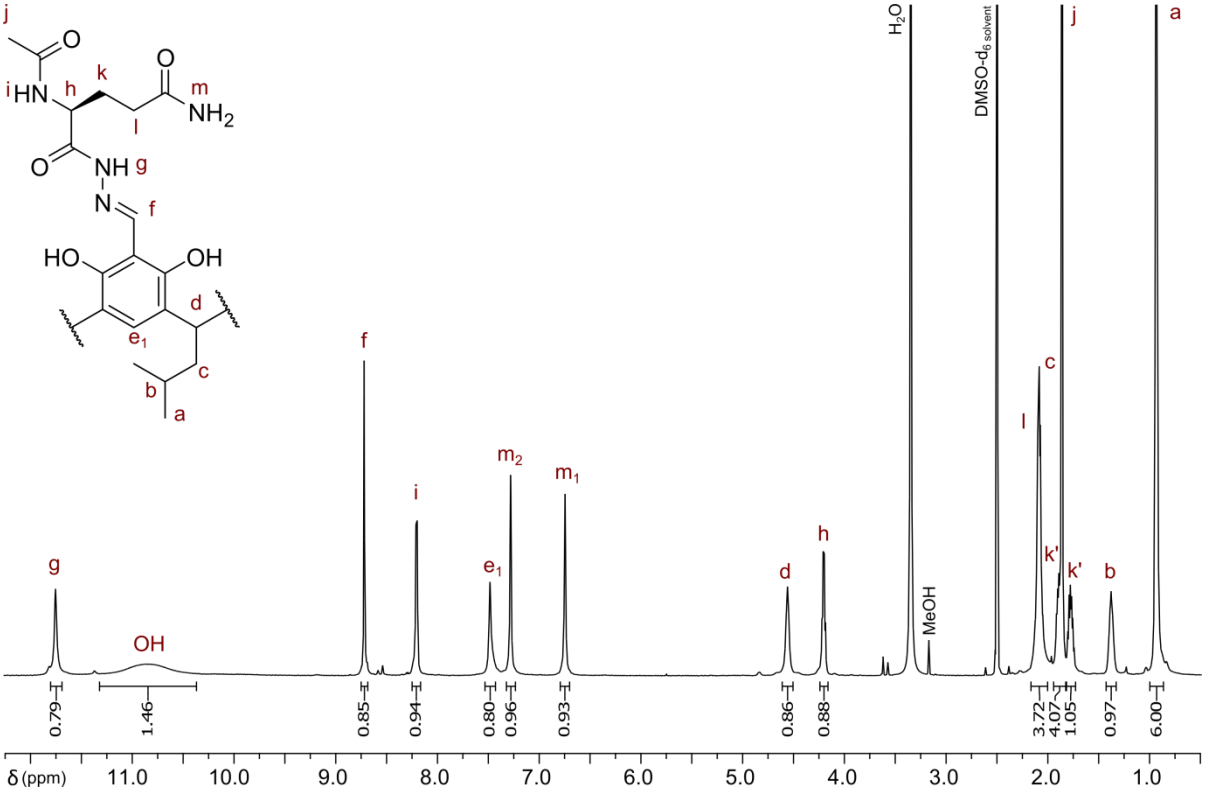

Fig. S9. ^{1}H NMR spectrum of **3a** (600 MHz, DMSO-d_6).

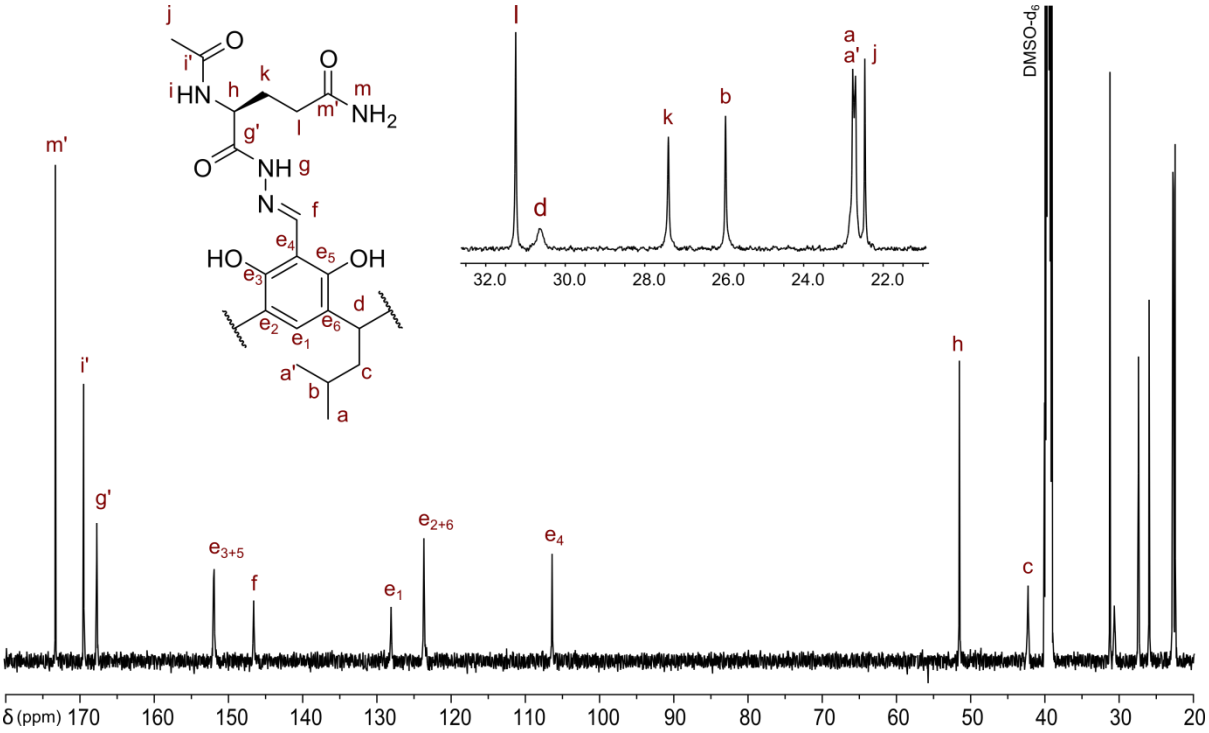

Fig. S10. ^{13}C NMR spectrum of **3a** (125 MHz, DMSO-d_6).

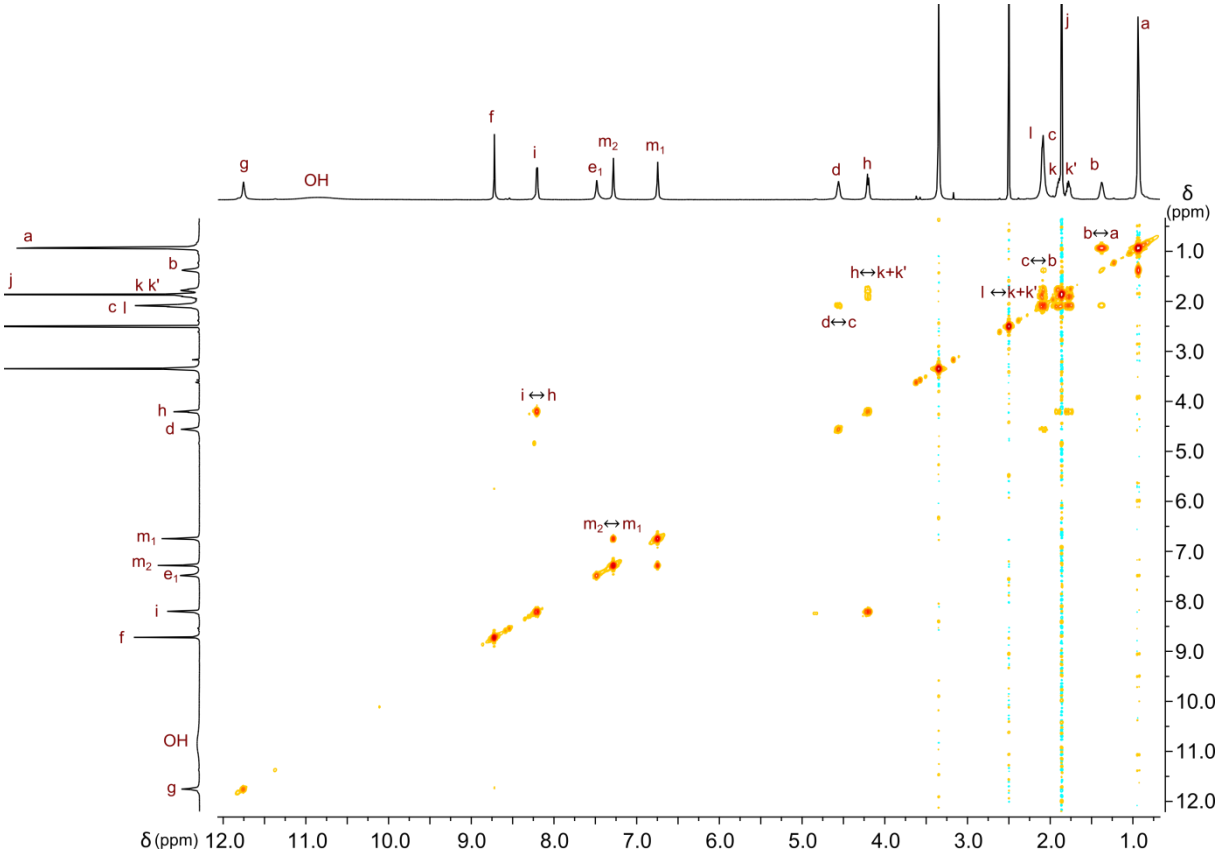

Fig. S11. ^{1}H-^{1}H COSY NMR spectrum of **3a** (600 MHz, DMSO-d_6).

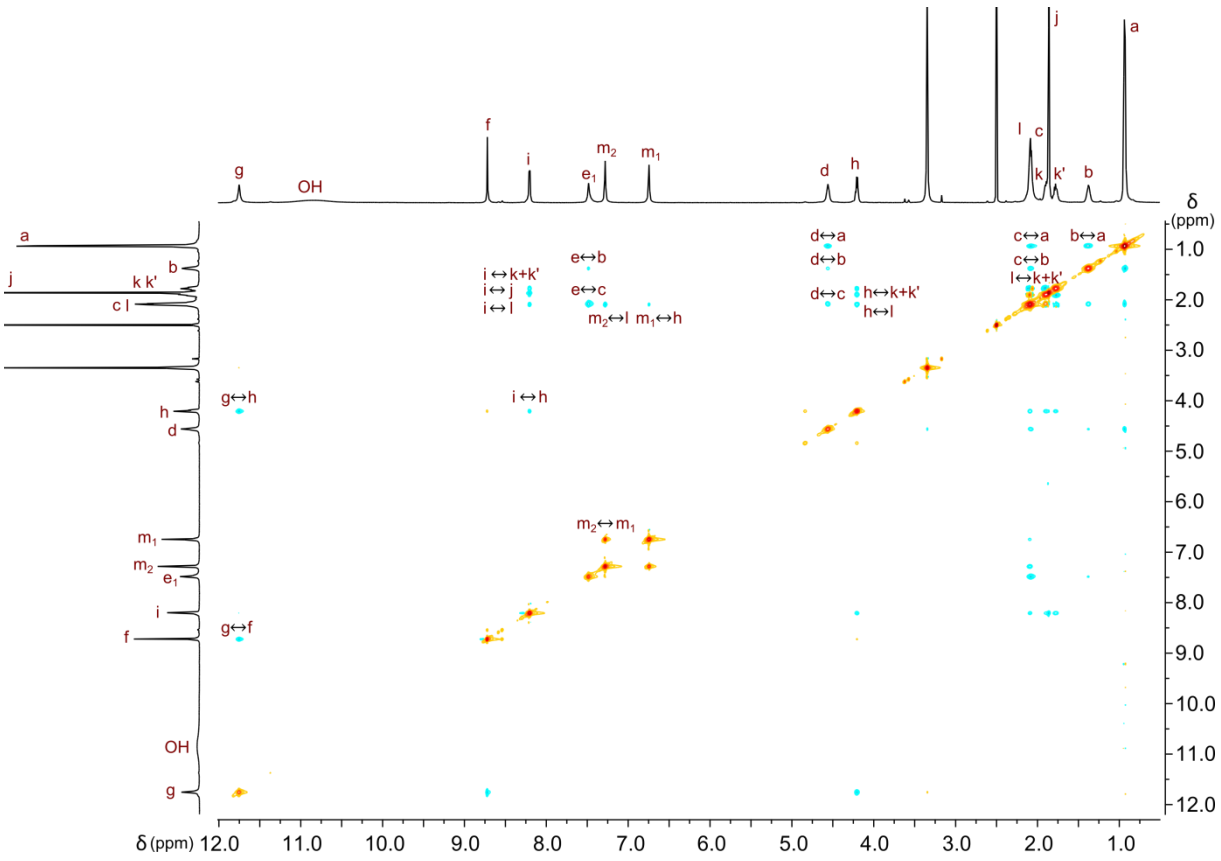

Fig. S12. ^{1}H-^{1}H ROESY NMR spectrum of **3a** (600 MHz, DMSO-d_6).

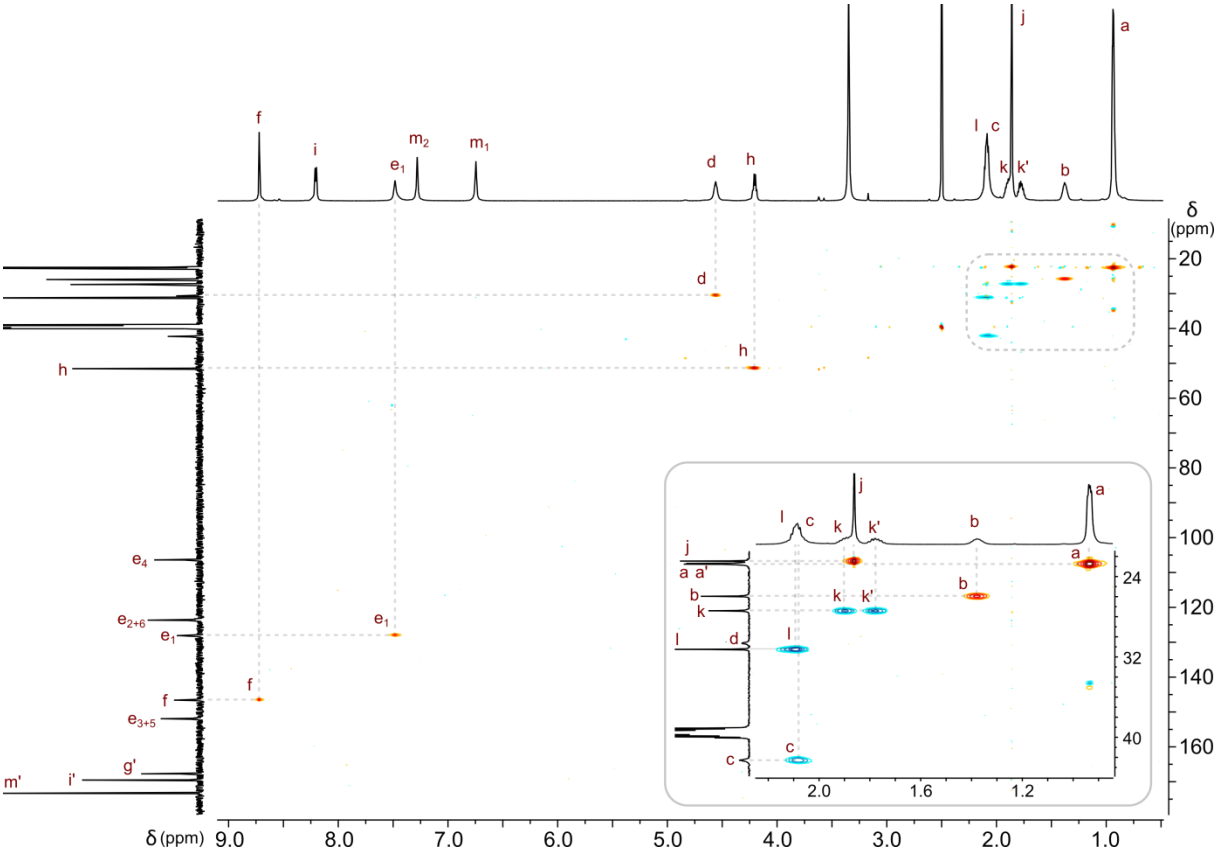

Fig. S13. ^{1}H-^{13}C HSQC NMR spectrum of **3a** (600 MHz, DMSO-d_6).

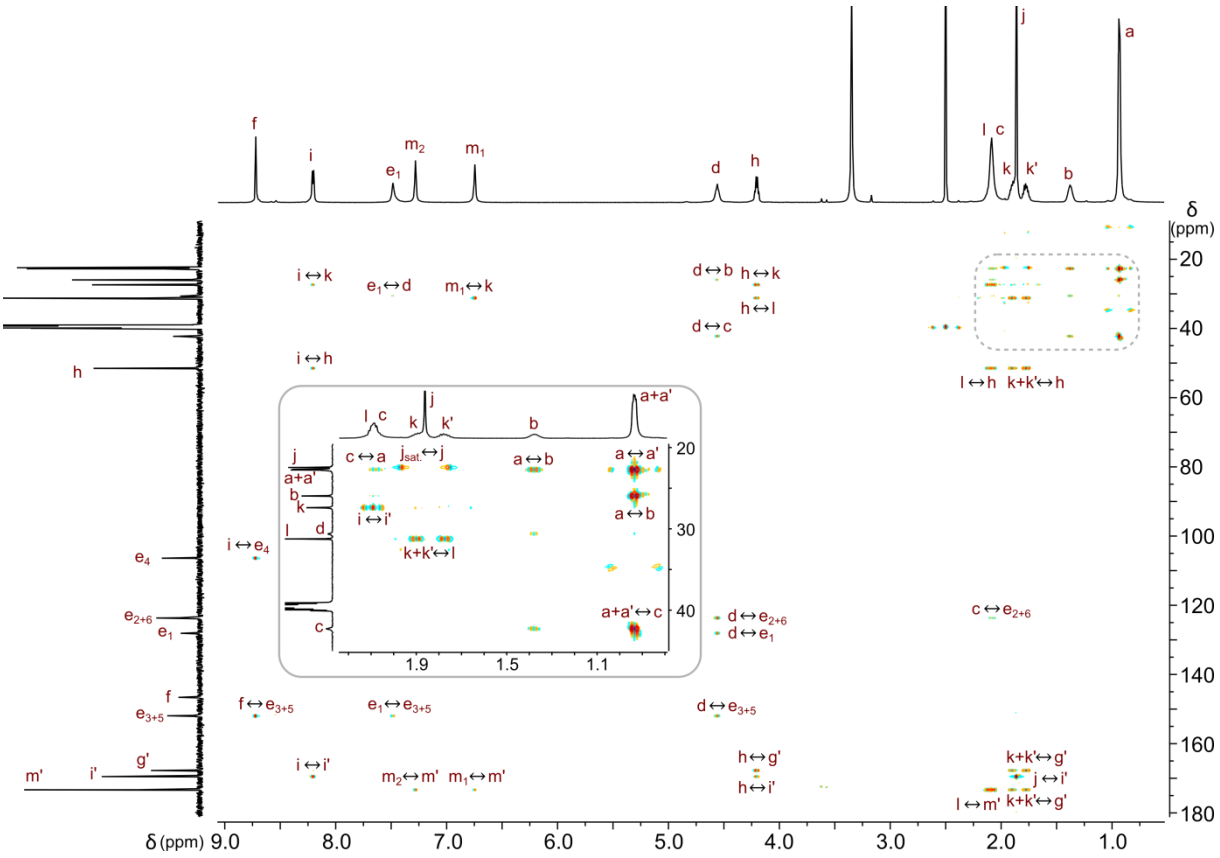

Fig. S14. ^{1}H-^{13}C HMBC NMR spectrum of **3a** (600 MHz, DMSO-d_6).

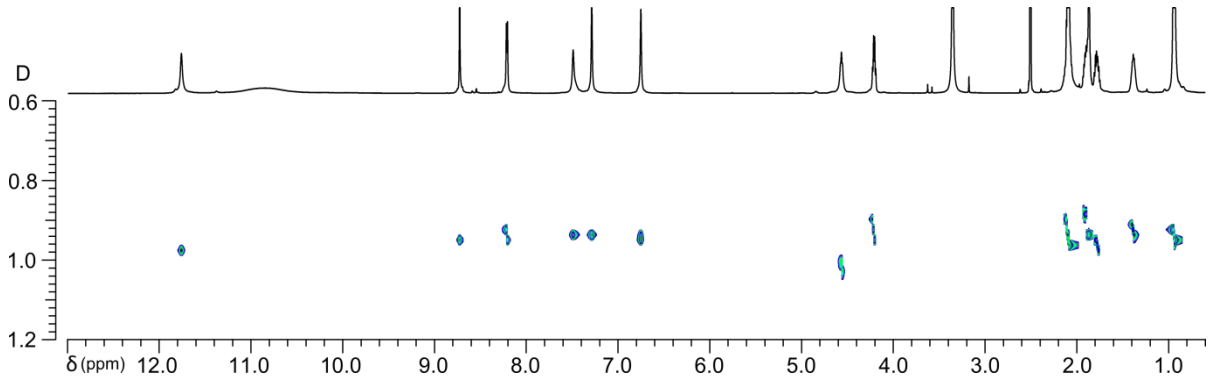

Fig. S15. DOSY NMR spectrum of **3a** (600 MHz, DMSO-d_6).

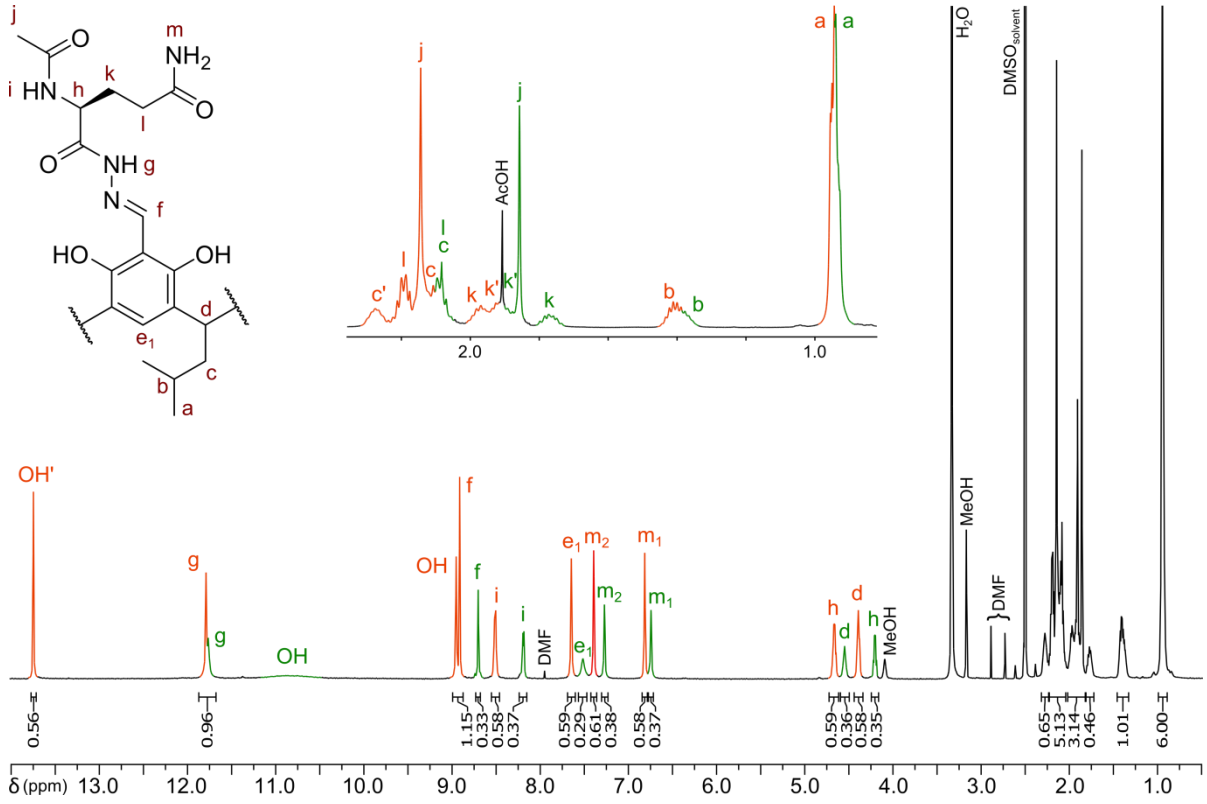

Fig. S16. ^{1}H NMR spectrum of (**3a**)$_2$⊃C_{60} (orange) and **3a** (green) (600 MHz, DMSO-d_6).

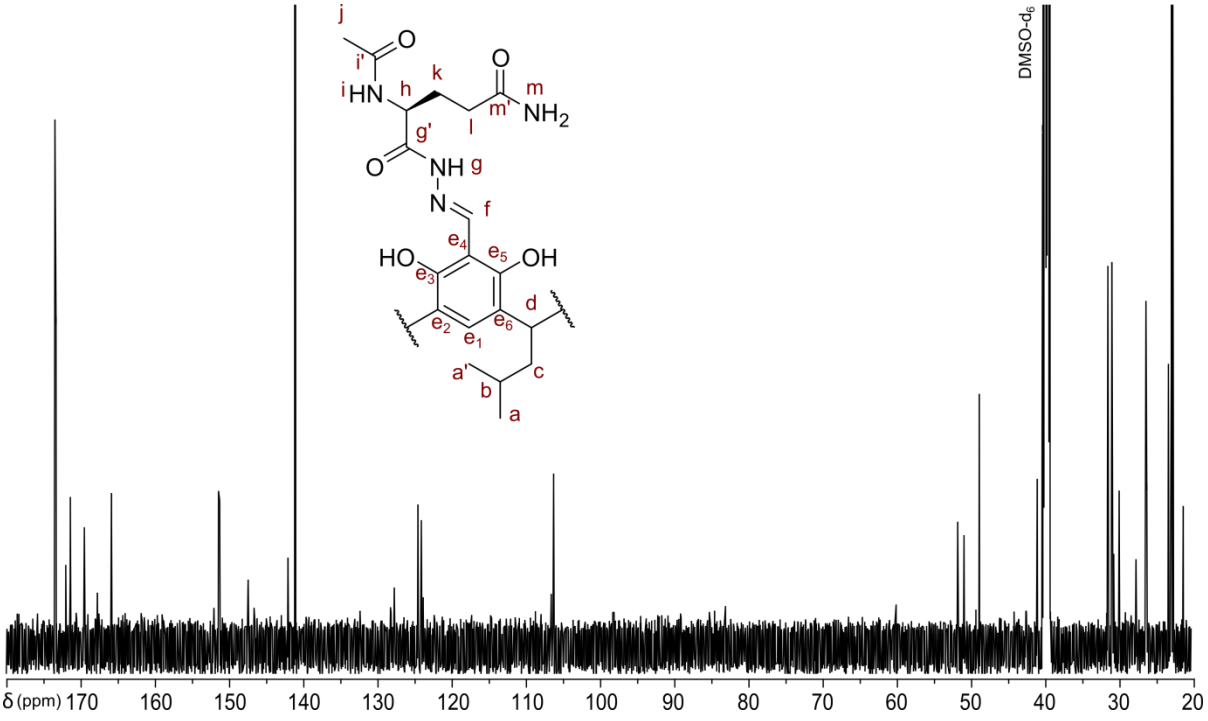

Fig. S17. ^{13}C NMR (125 MHz, DMSO-d_6) spectrum of a mixture of (**3a**)$_2$⊃C_{60} and **3a**.

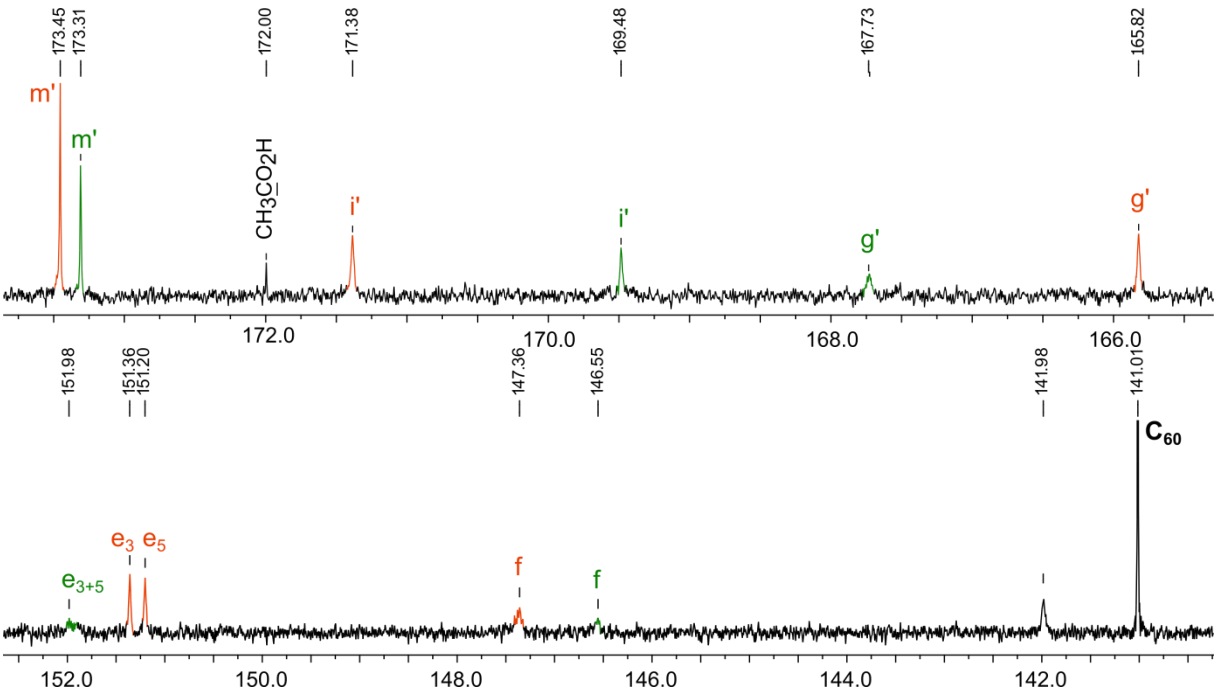

Fig. S18. Expanded regions of ^{13}C NMR spectrum of a mixture of (**3a**)$_2$⊃C_{60} (orange) and **3a** (green) (125 MHz, DMSO-d_6).

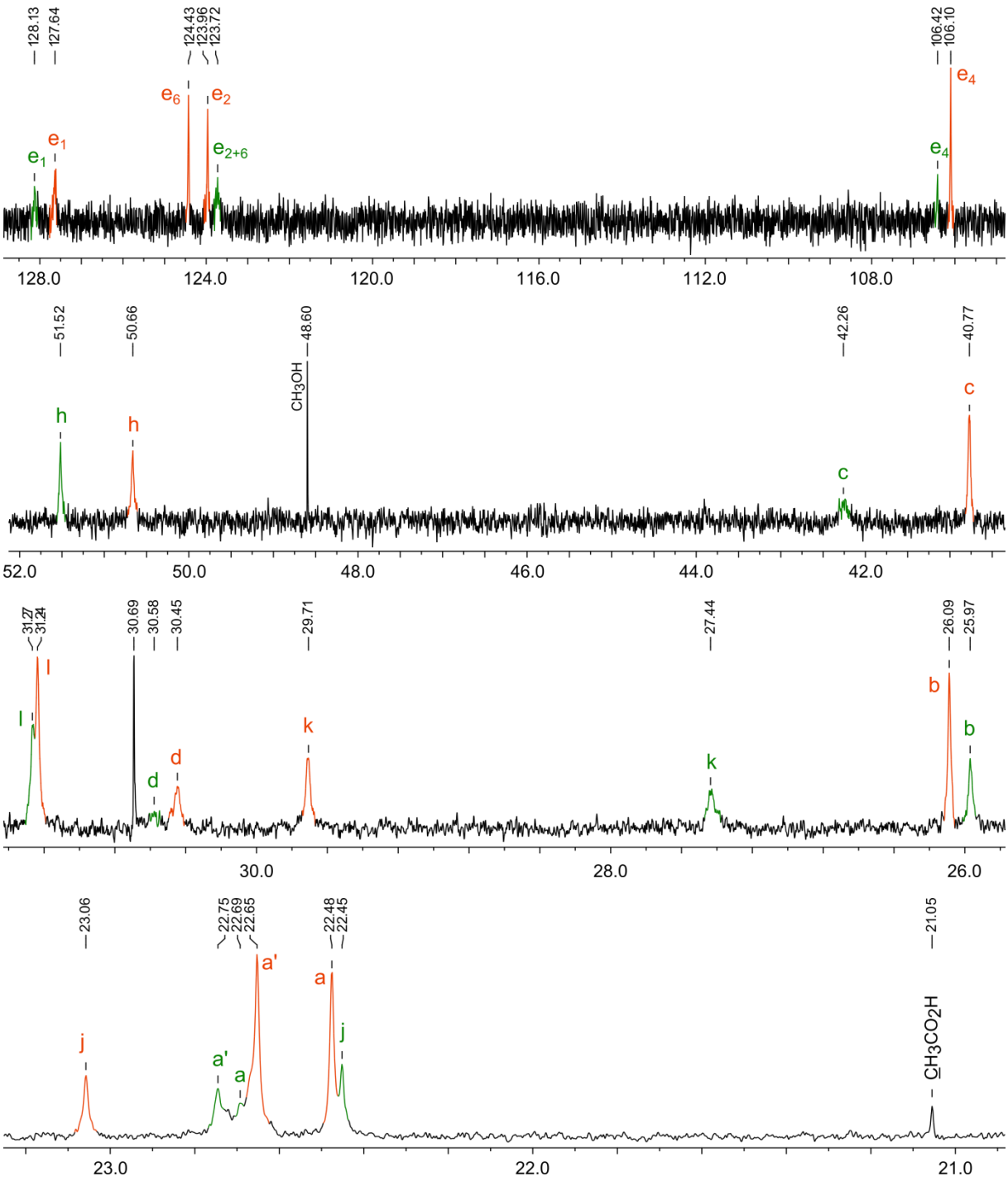

Fig. S19. Expanded regions of ^{13}C NMR spectrum of a mixture of (**3a**)$_2$⊃C_{60} (orange) and **3a** (green) (125 MHz, DMSO-d_6).

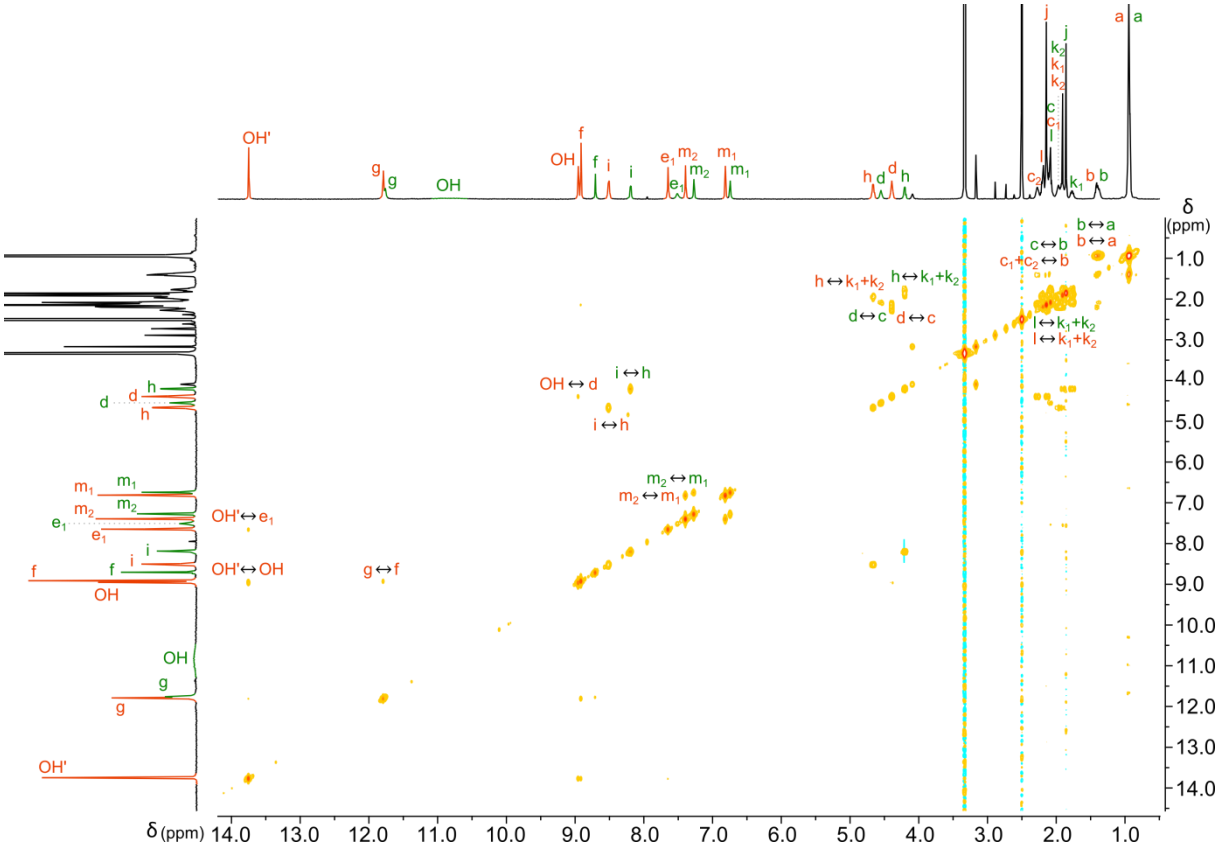

Fig. S20. ^{1}H-^{1}H COSY NMR spectrum of a mixture of (**3a**)$_2$⊃C_{60} (orange) and **3a** (green) (600 MHz, DMSO-d_6).

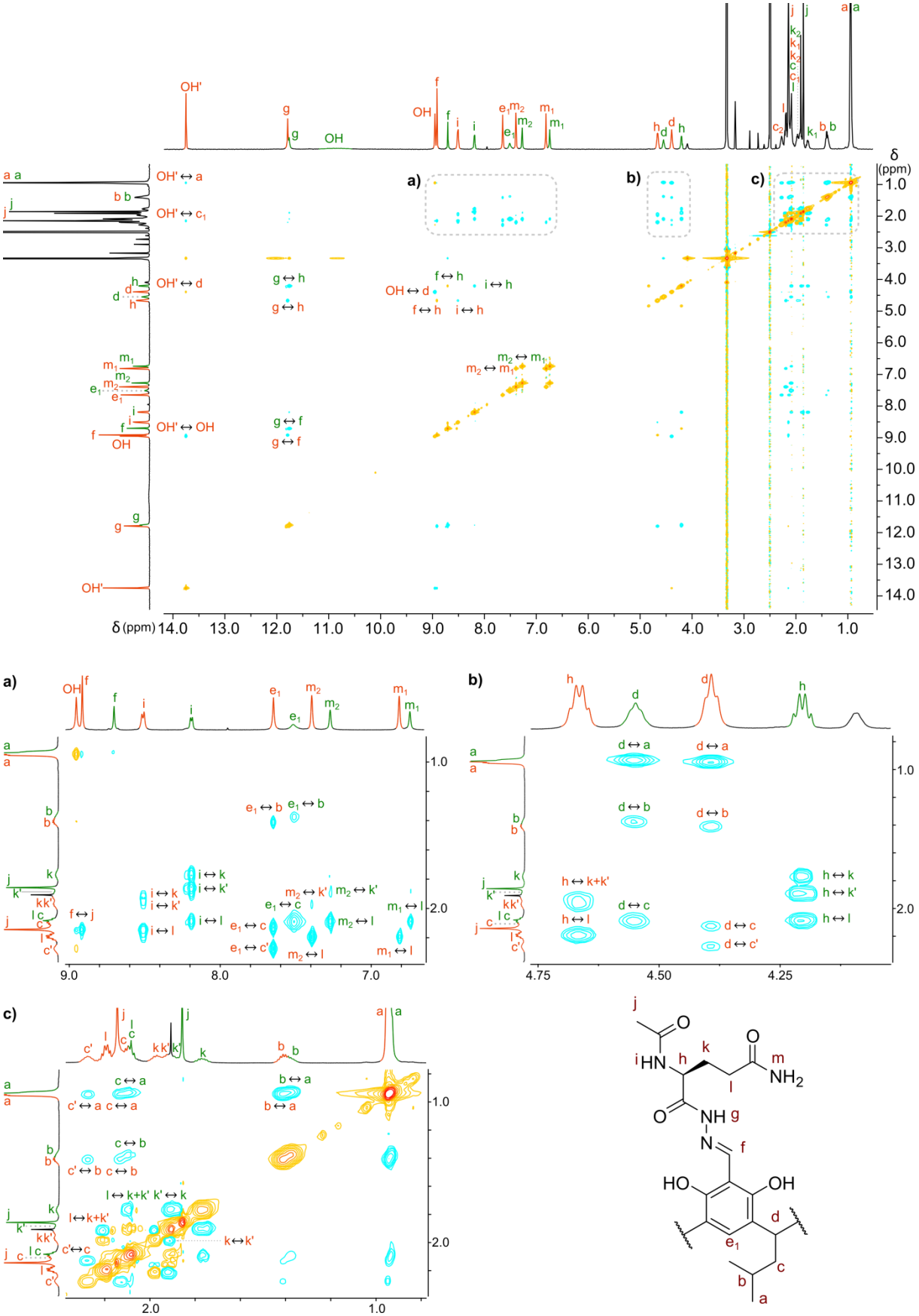

Fig. S21. ^{1}H-^{1}H ROESY NMR spectrum of a mixture of (**3a**)$_2$⊃C_{60} (orange) and **3a** (green) (600 MHz, DMSO-d_6).

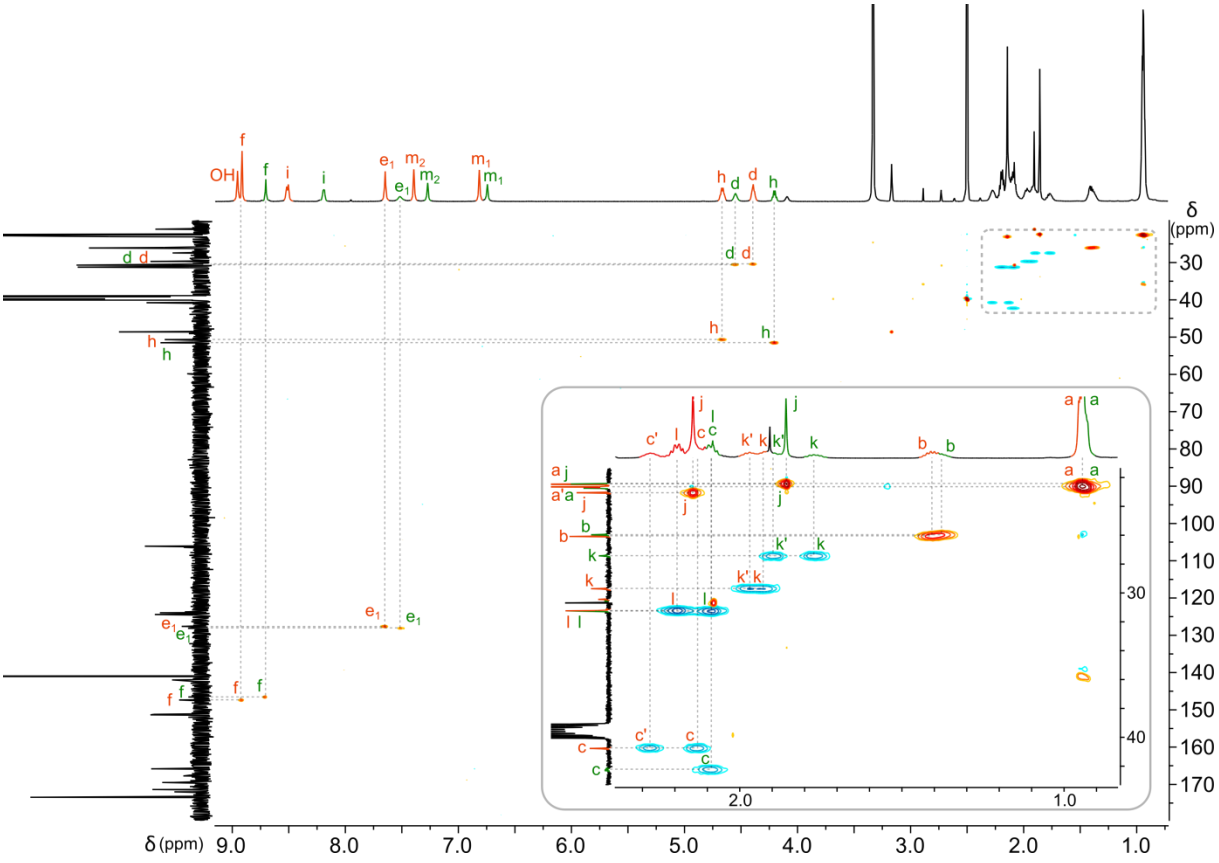

Fig. S22. ^{1}H-^{13}C HSQC NMR spectrum of a mixture of (**3a**)$_2$⊃C_{60} (orange) and **3a** (green) (600 MHz, DMSO-d_6).

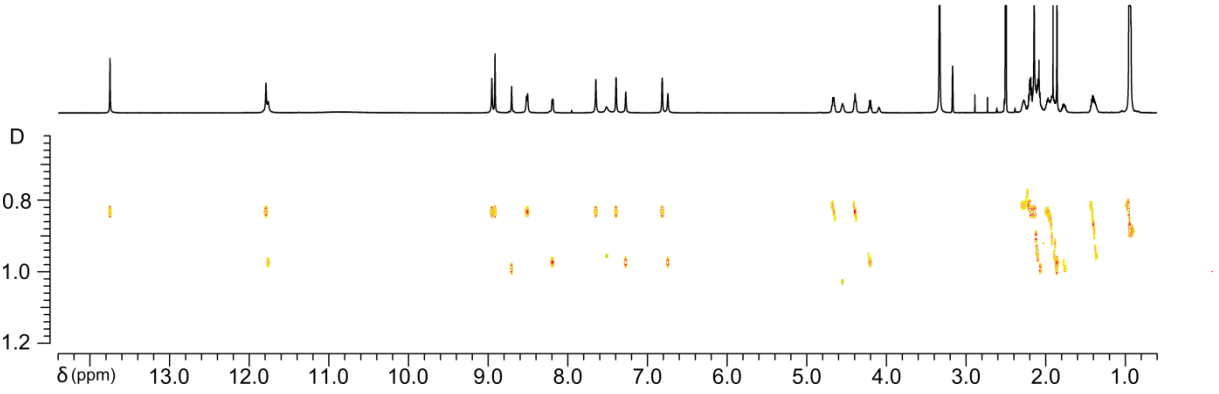

Fig. S23. DOSY NMR spectrum of a mixture of (**3a**)$_2$⊃C_{60} and **3a** (600 MHz, DMSO-d_6).

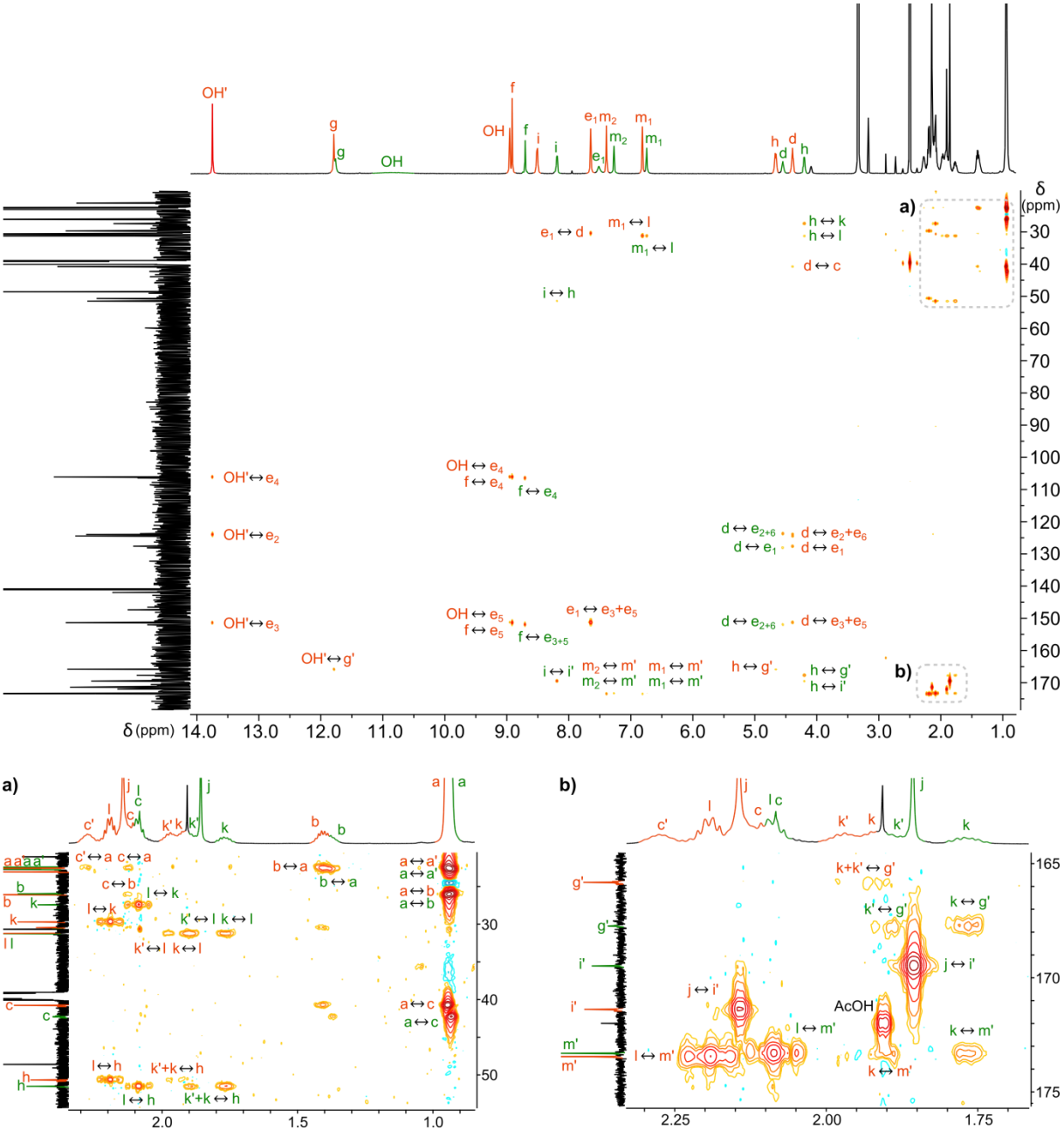

Fig. S24. ^{1}H-^{13}C HMBC NMR spectrum of a mixture of (**3a**)$_2$⊃C_{60} (orange) and **3a** (green) (600 MHz, DMSO-d_6).

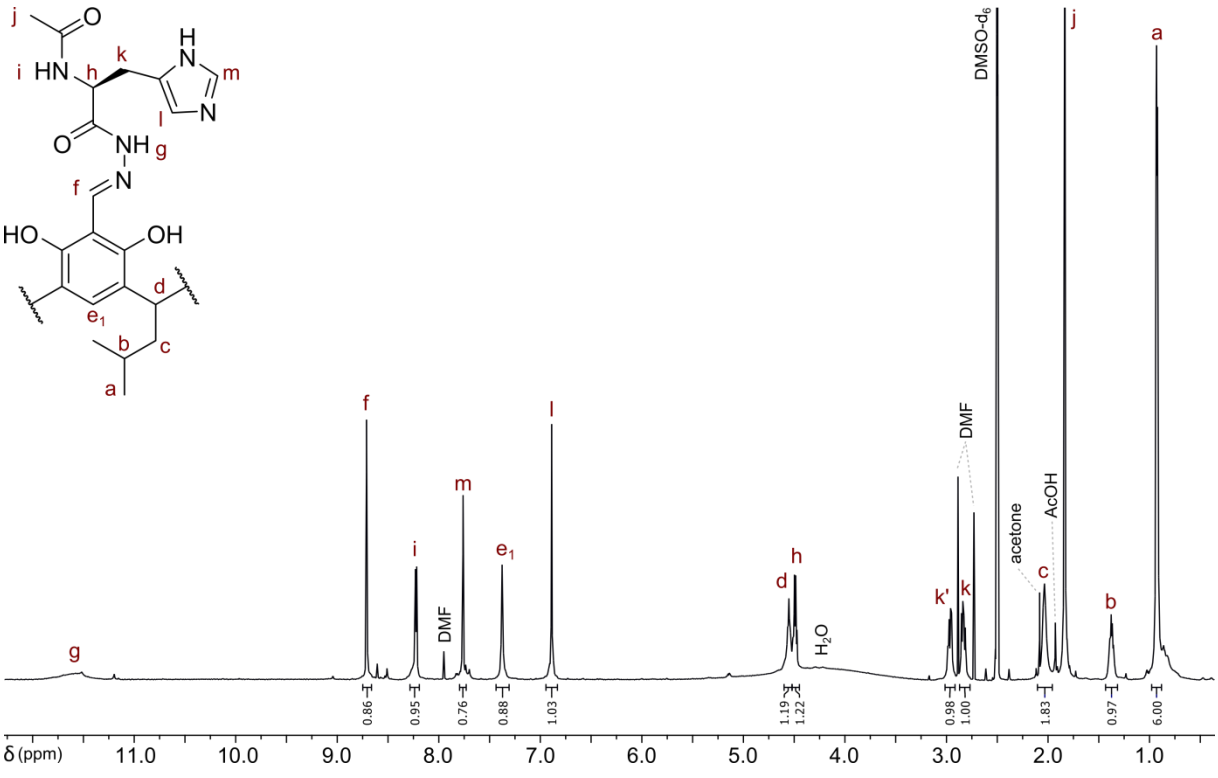

Fig. S25. ^{1}H NMR spectrum of **3b** (600 MHz, DMSO-d_6).

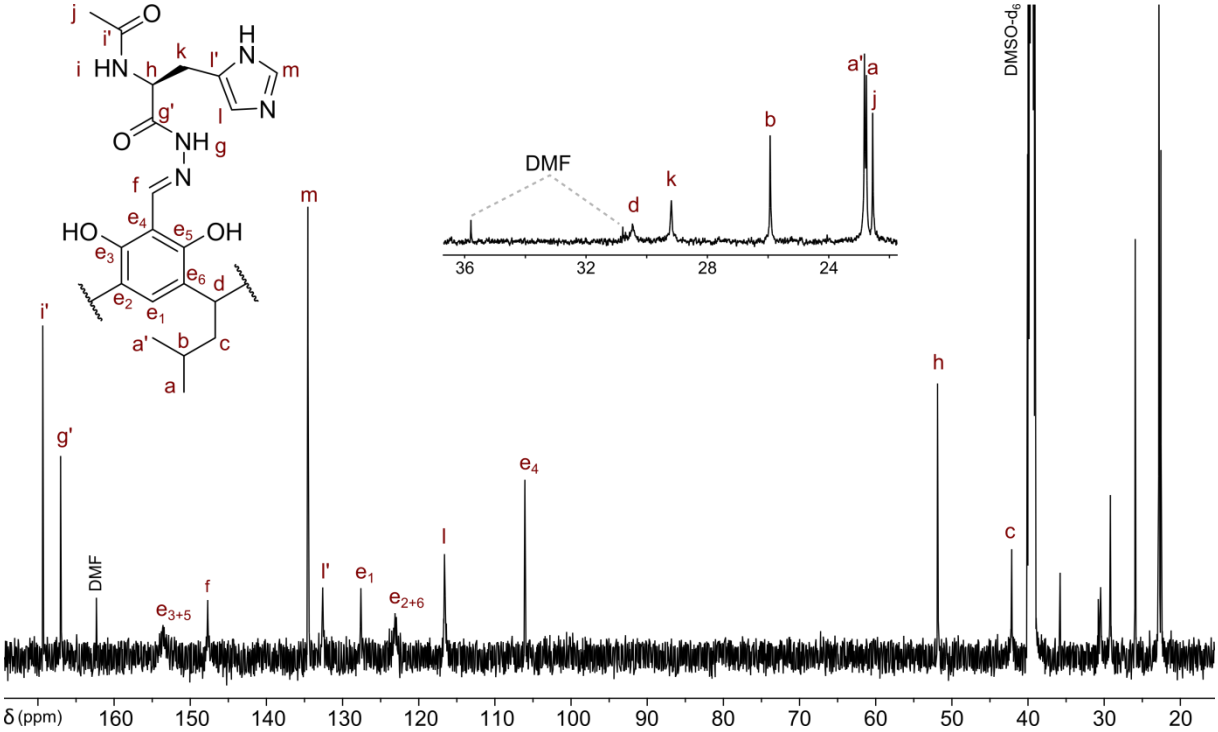

Fig. S26. ^{13}C NMR spectrum of **3b** (125 MHz, DMSO-d_6).

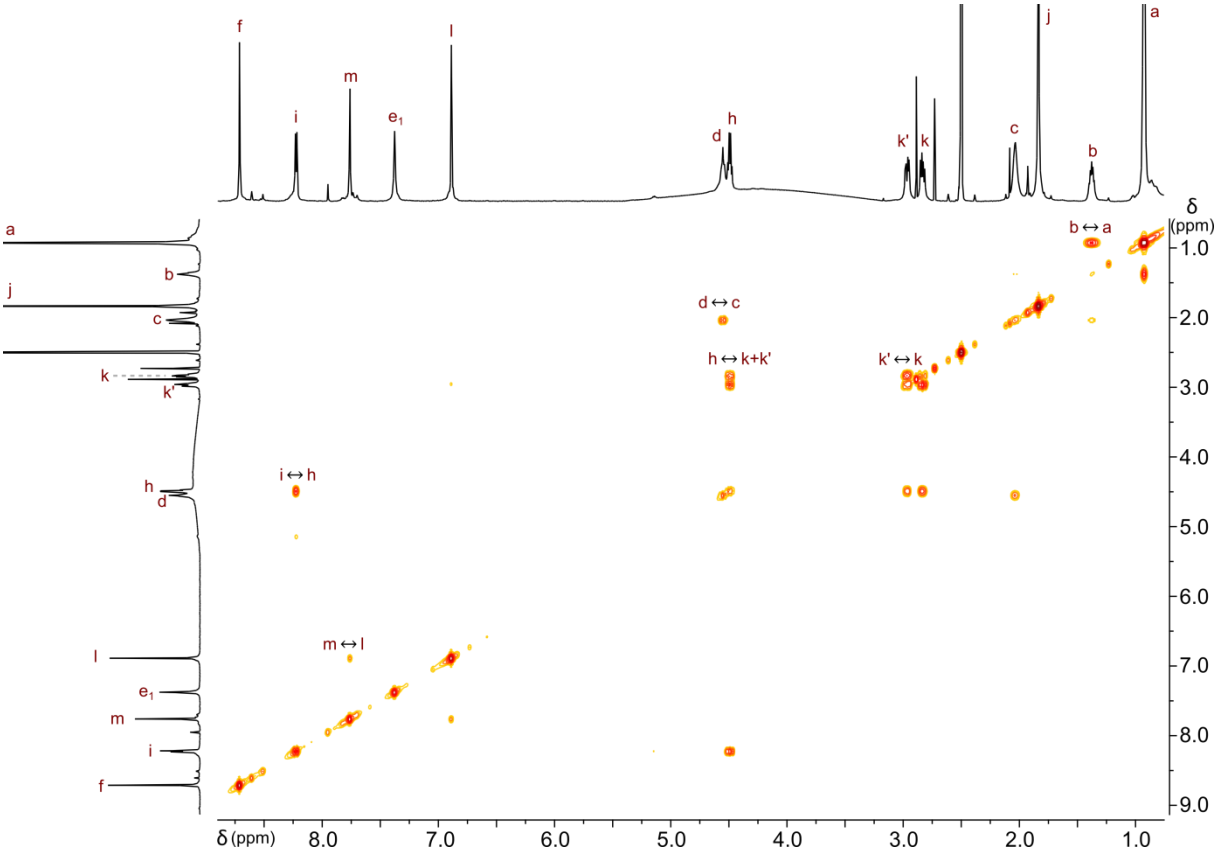

Fig. S27. ^{1}H-^{1}H COSY NMR spectrum of **3b** (600 MHz, DMSO-d_6).

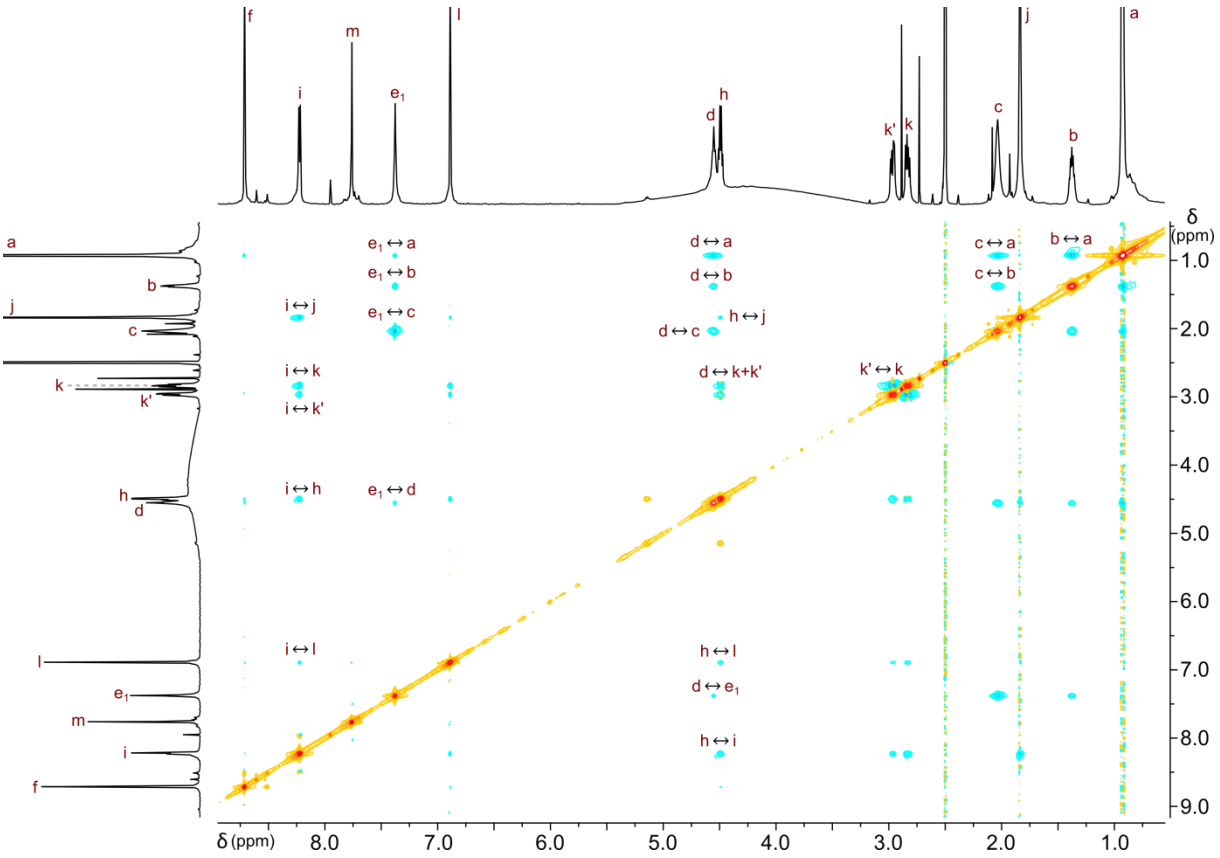

Fig. S28. ^{1}H-^{1}H ROESY NMR spectrum of **3b** (600 MHz, DMSO-d_6).

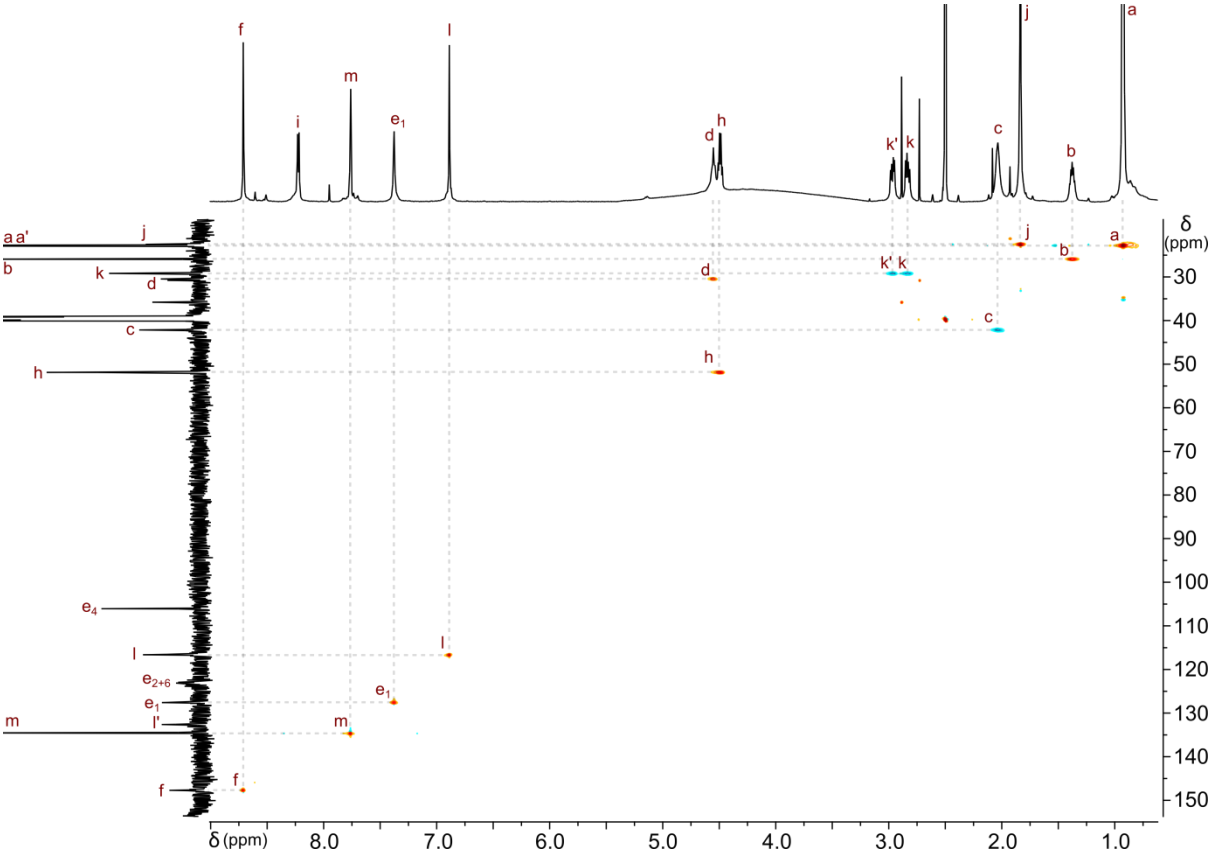

Fig. S29. ^{1}H-^{13}C HSQC NMR spectrum of **3b** (600 MHz, DMSO-d_6).

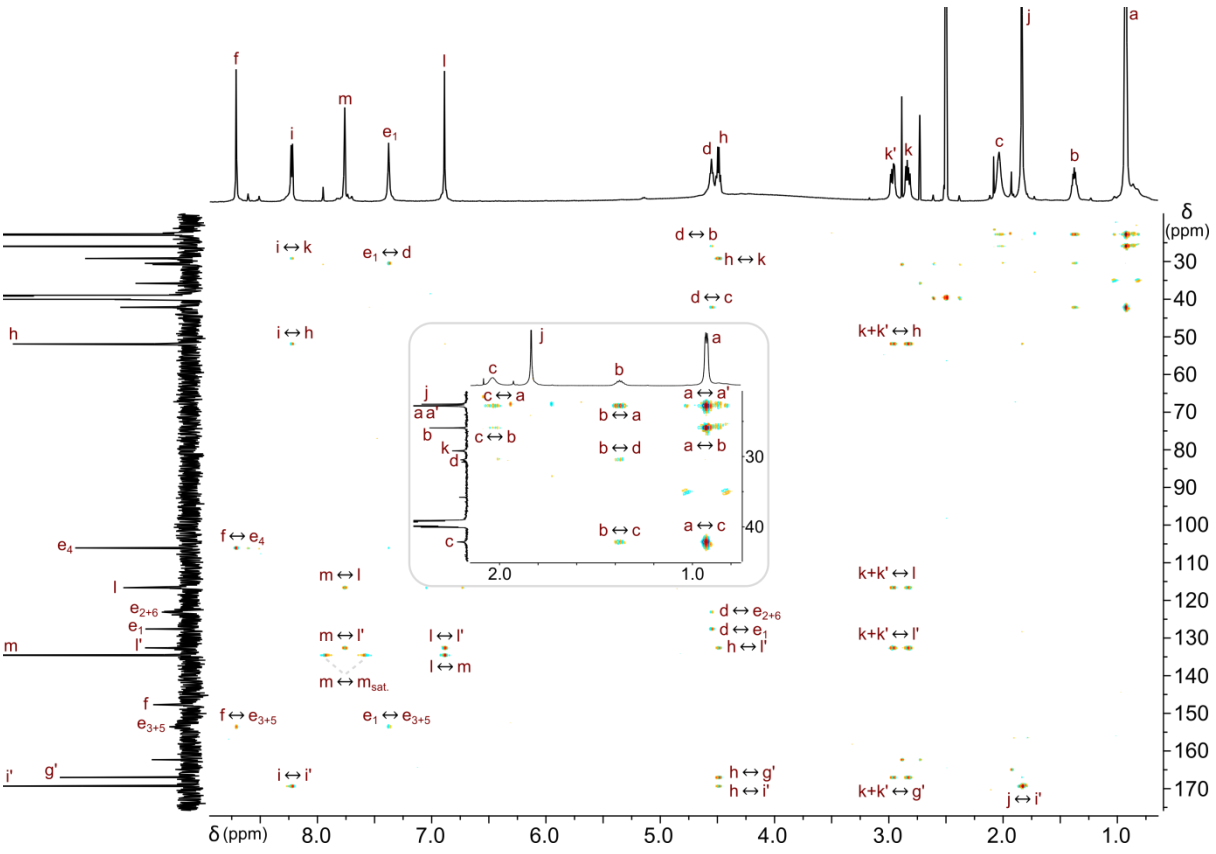

Fig. S30. ^{1}H-^{13}C HMBC NMR spectrum of **3b** (600 MHz, DMSO-d_6).

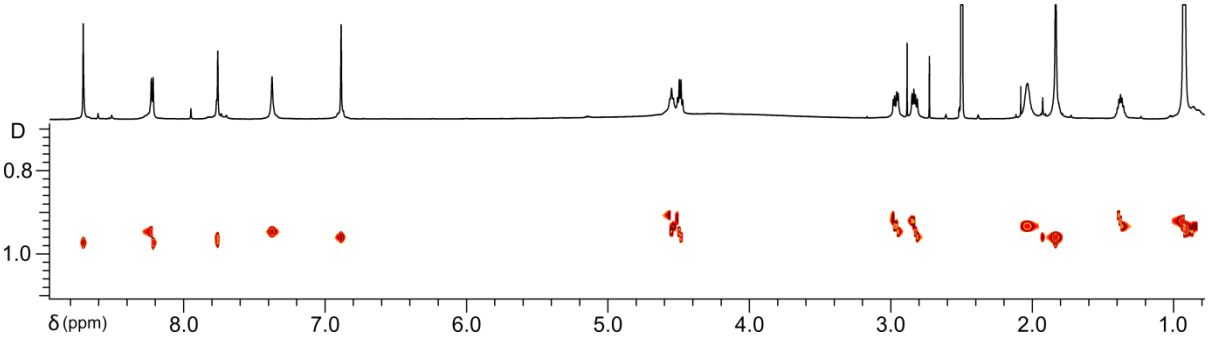

Fig. S31. DOSY NMR spectrum of **3b** (600 MHz, DMSO-d_6).

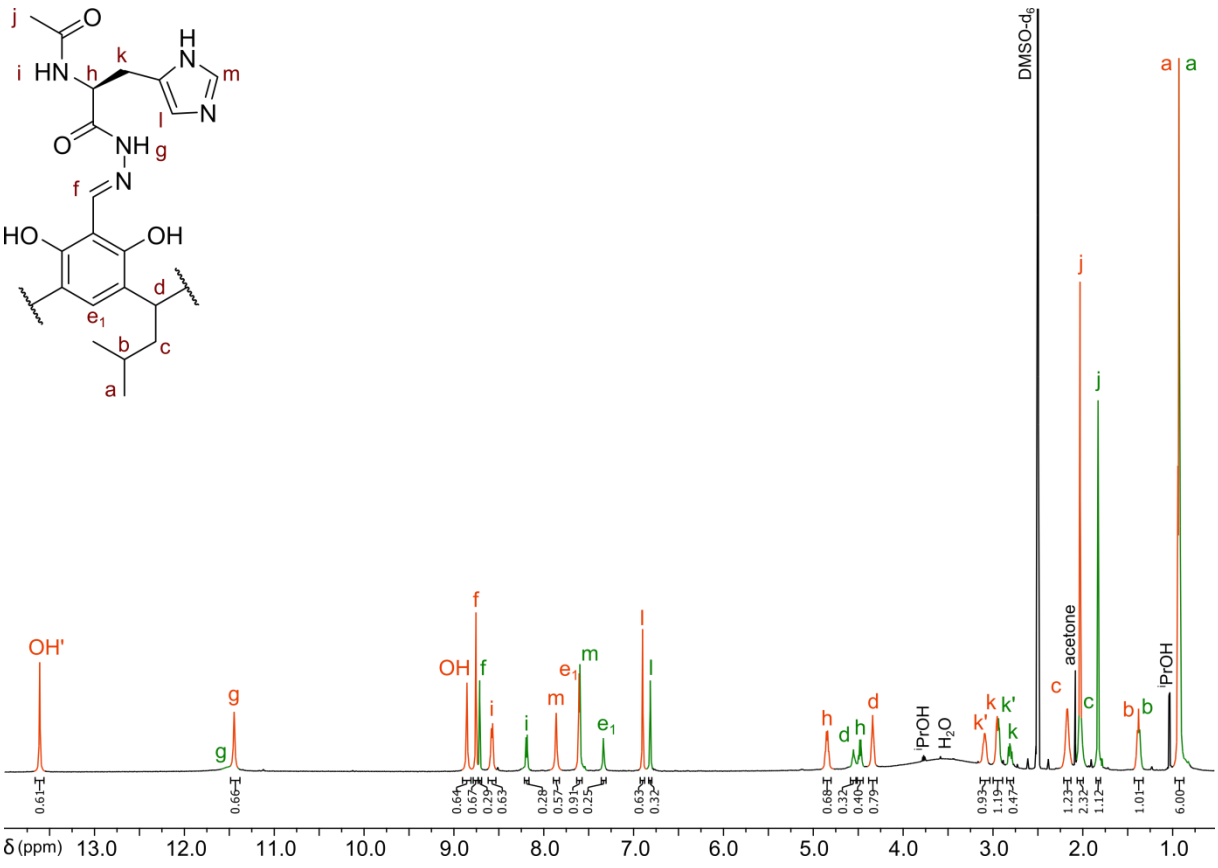

Fig. S32. ^{1}H NMR spectrum of (**3b**)$_2$⊃C_{60} (orange) and **3b** (green) (600 MHz, DMSO-d_6).

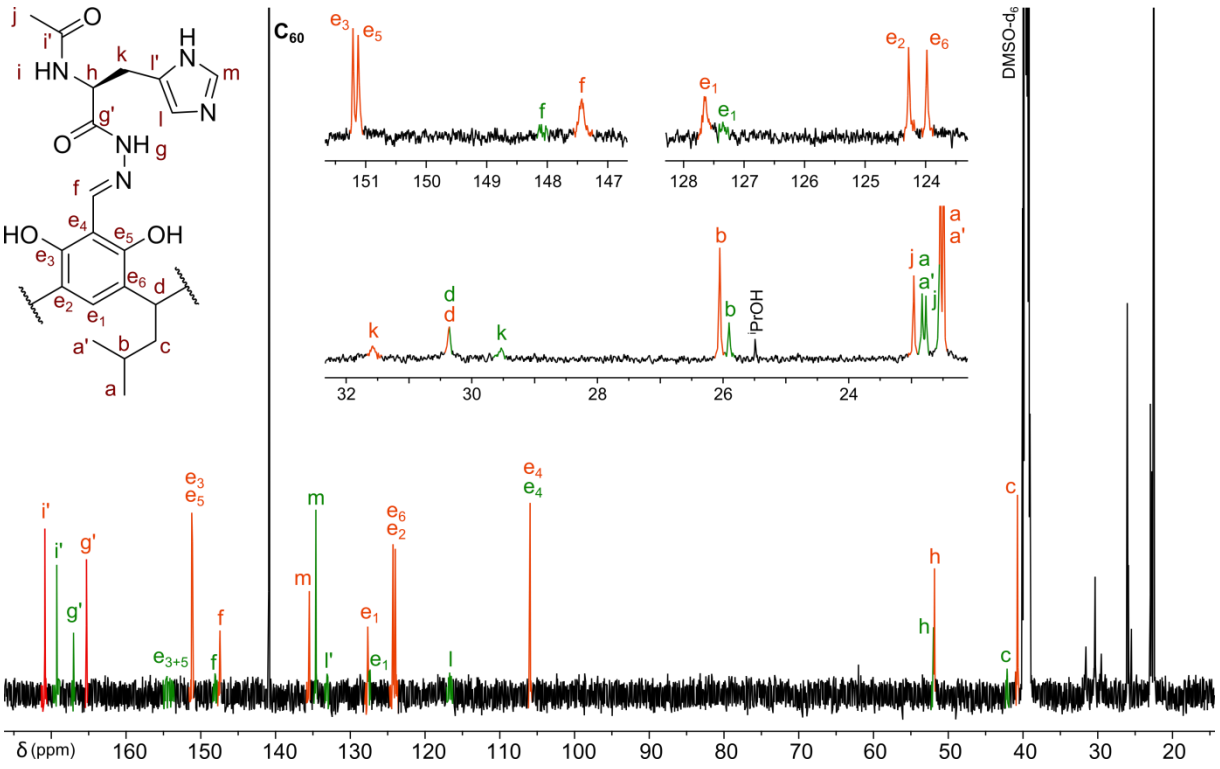

Fig. S33. ^{13}C NMR spectrum of a mixture of (**3b**)$_2$⊃C_{60} (orange) and **3b** (green) (125 MHz, DMSO-d$_6$).

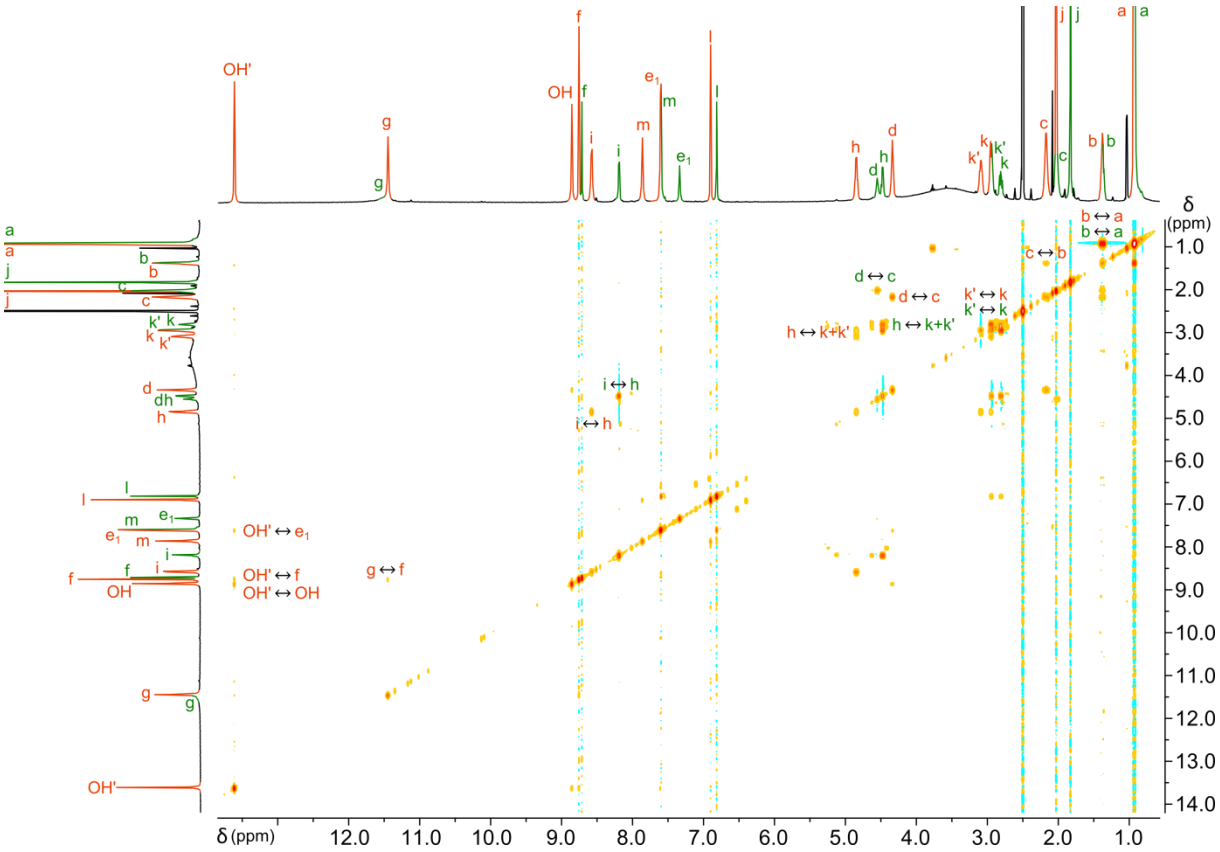

Fig. S34. ^{1}H-^{1}H COSY NMR spectrum of a mixture of (**3b**)$_2$⊃C_{60} (orange) and **3b** (green) (600 MHz, DMSO-d$_6$).

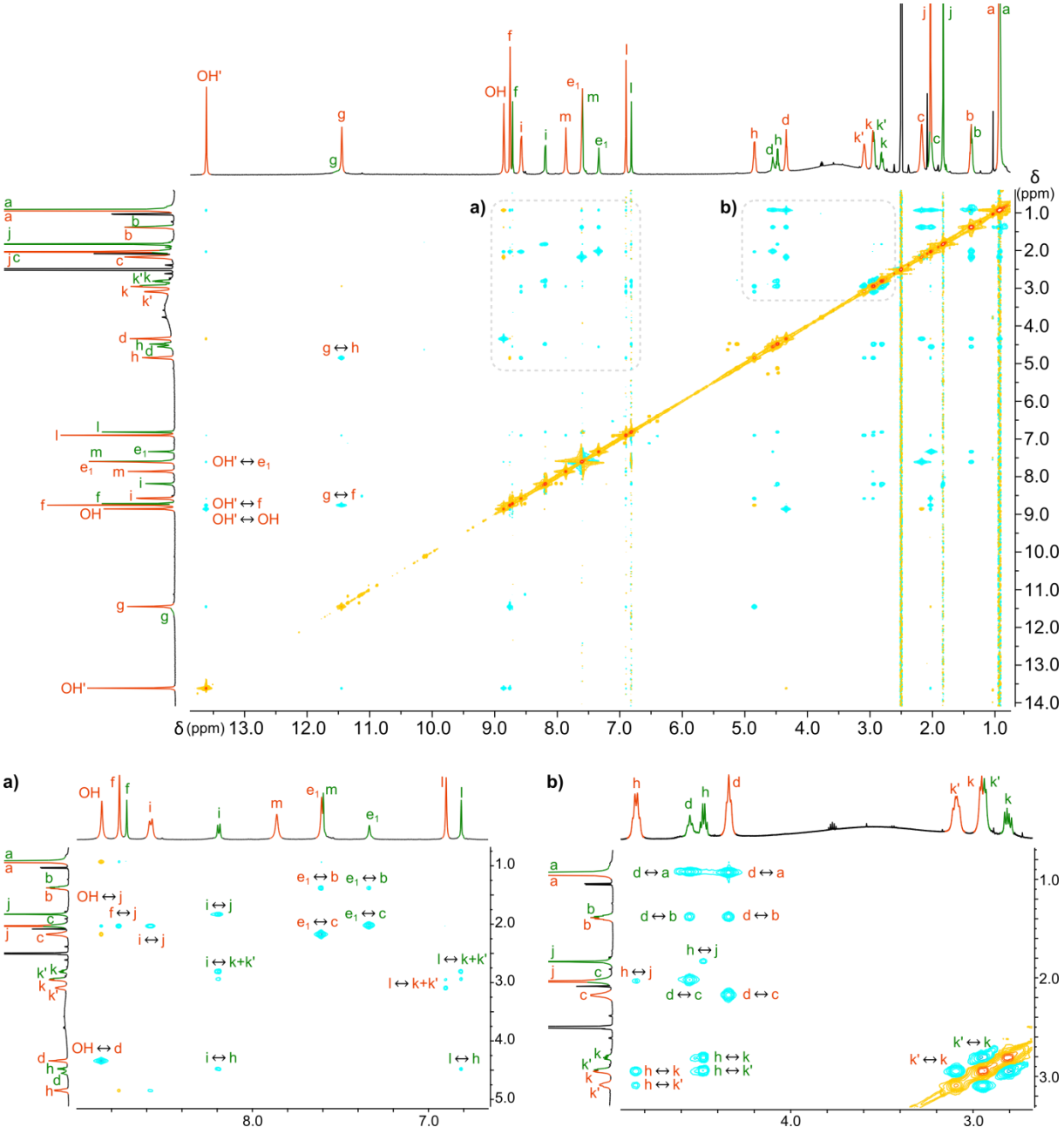

Fig. S35. ^{1}H-^{1}H ROESY NMR spectrum of a mixture of (**3b**)$_2$⊃C_{60} (orange) and **3b** (green) (600 MHz, DMSO-d_6).

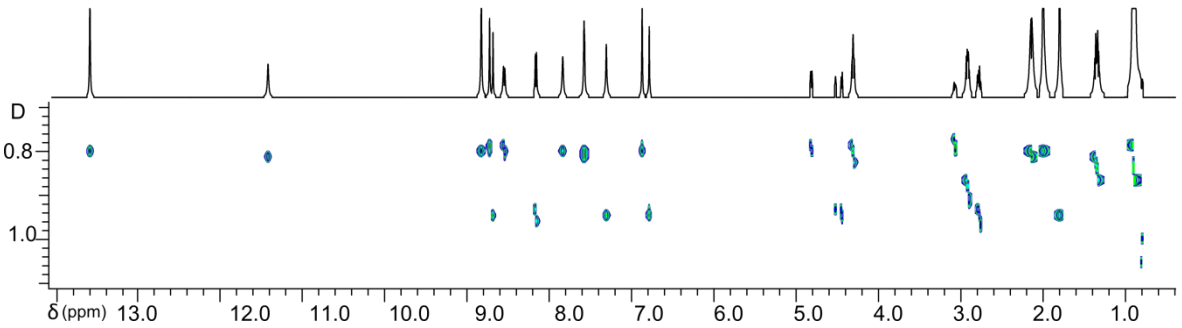

Fig. S36. DOSY NMR spectrum of a mixture of (**3b**)$_2$⊃C_{60} and **3b**(600 MHz, DMSO-d_6).

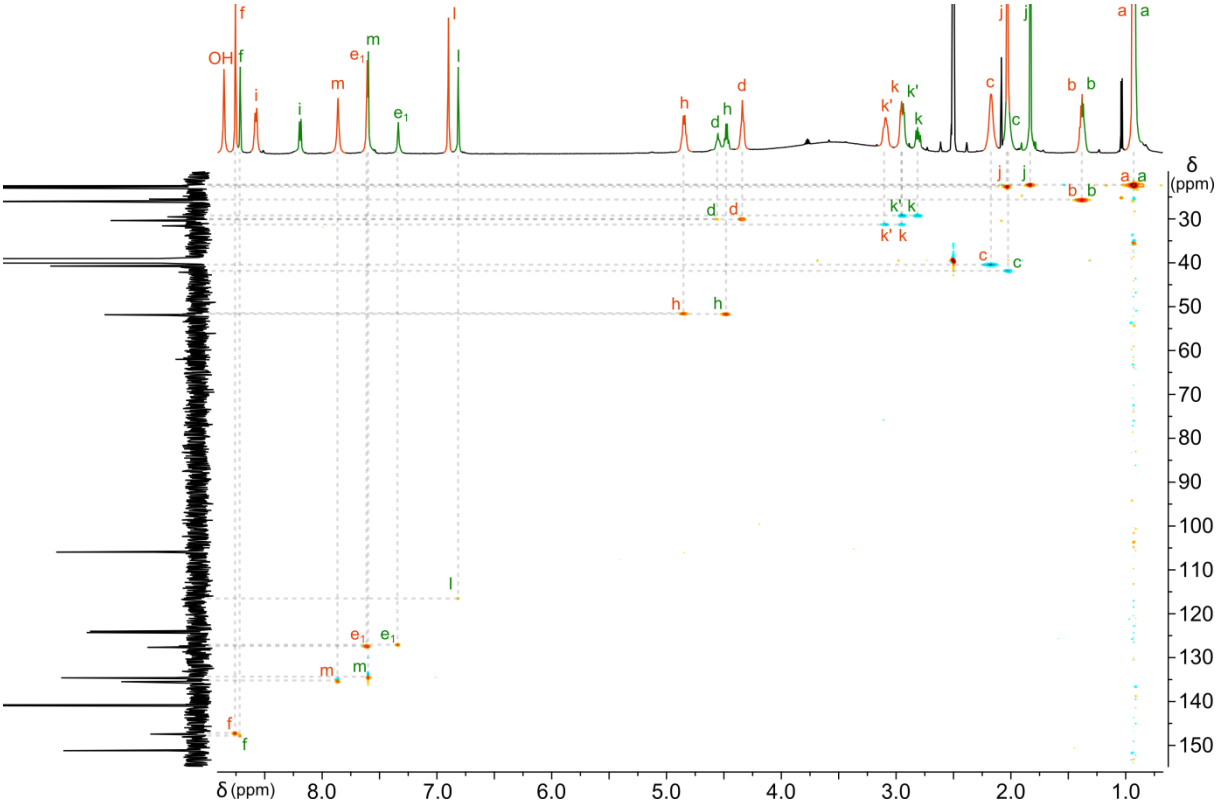

Fig. S37. ^{1}H-^{13}C HSQC NMR spectrum of a mixture of (**3b**)$_2$⊃C_{60} (orange) and **3b** (green) (600 MHz, DMSO-d_6).

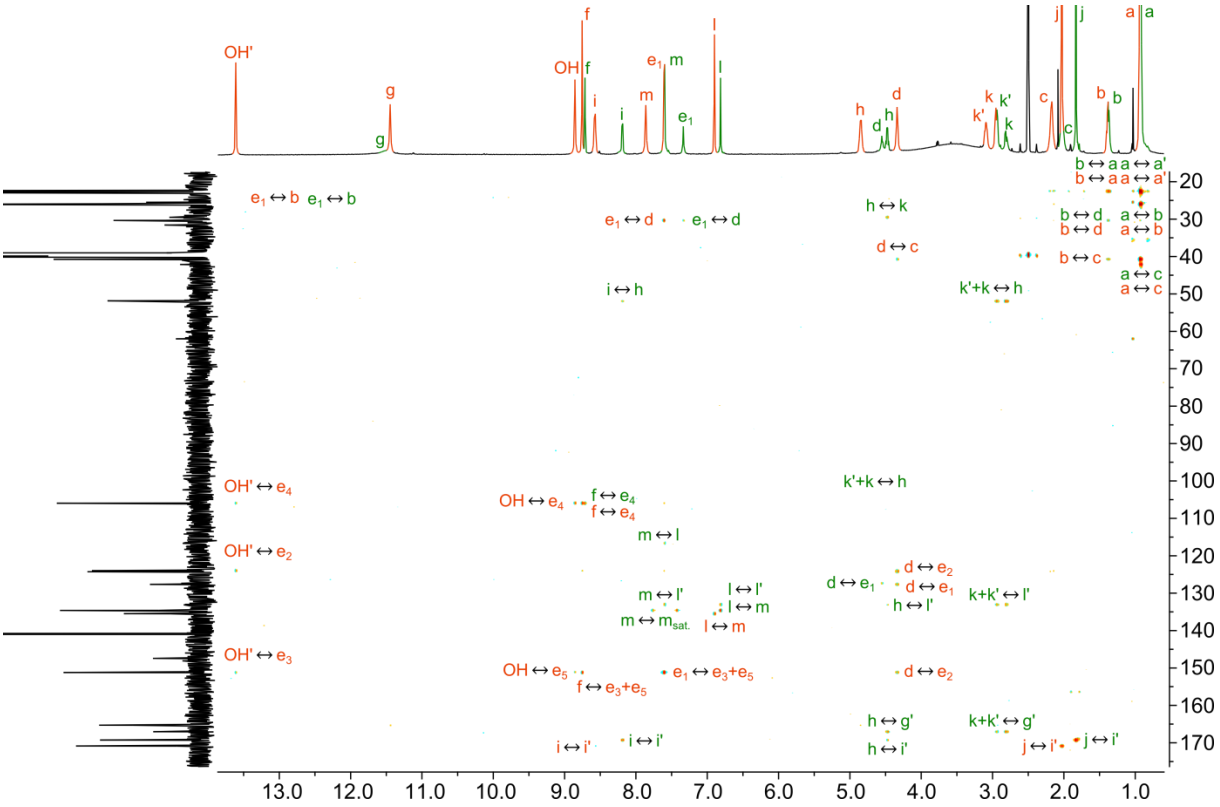

Fig. S38. ^{1}H-^{13}C HMBC NMR spectrum of a mixture of (**3b**)$_2$⊃C_{60} (orange) and **3b** (green) (600 MHz, DMSO-d_6).

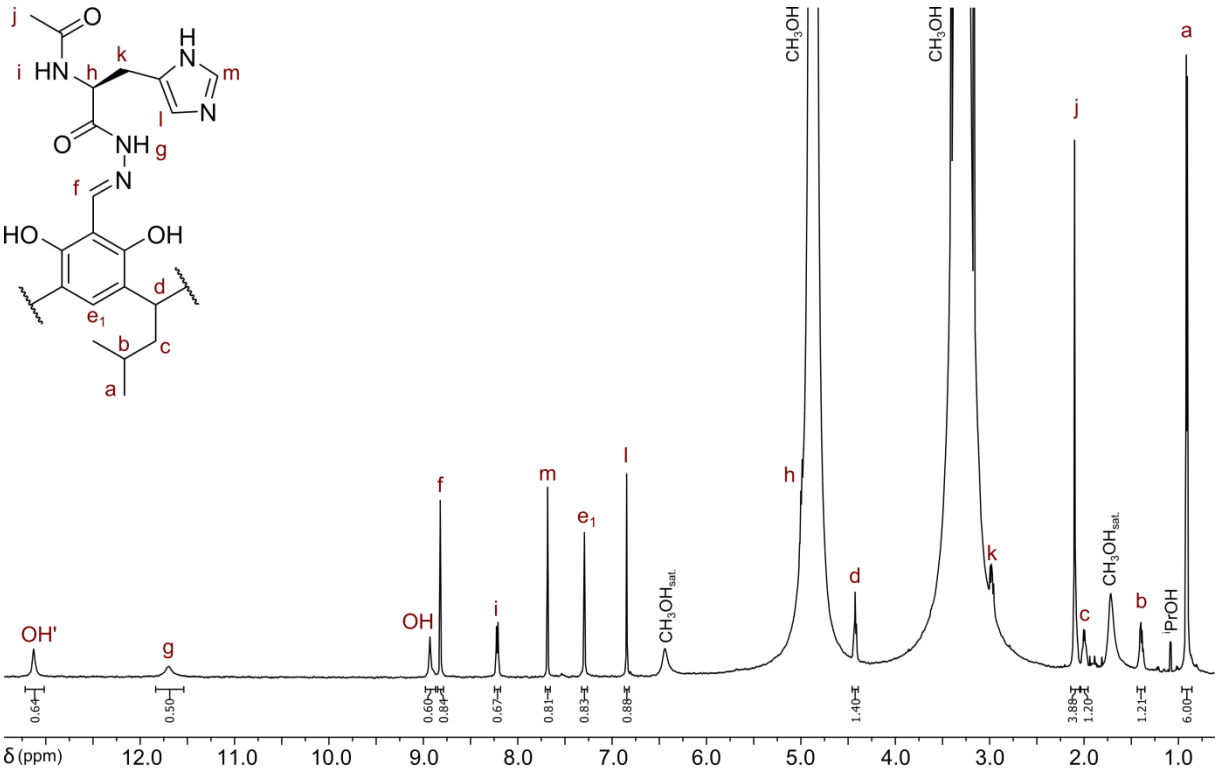

Fig. S39. ^{1}H NMR spectrum of (**3b**)$_2$⊃C_{60}(600 MHz, CD_3OD:CH_3OH, 1:9, *v*:*v* without presaturation).

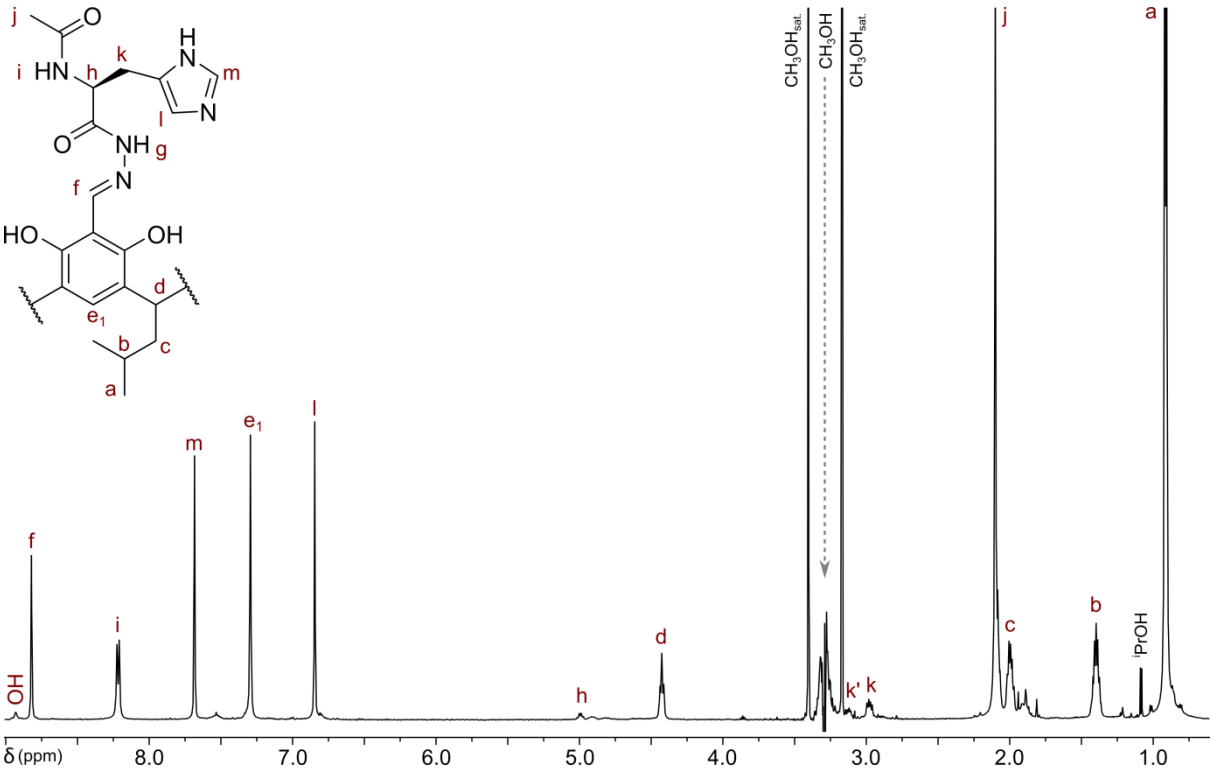

Fig. S40. ^{1}H NMR spectrum of (**3b**)$_2$⊃C_{60} (600 MHz, CD_3OD:CH_3OH, 1:9, *v*:*v* with presaturation of CH_3OH signal).

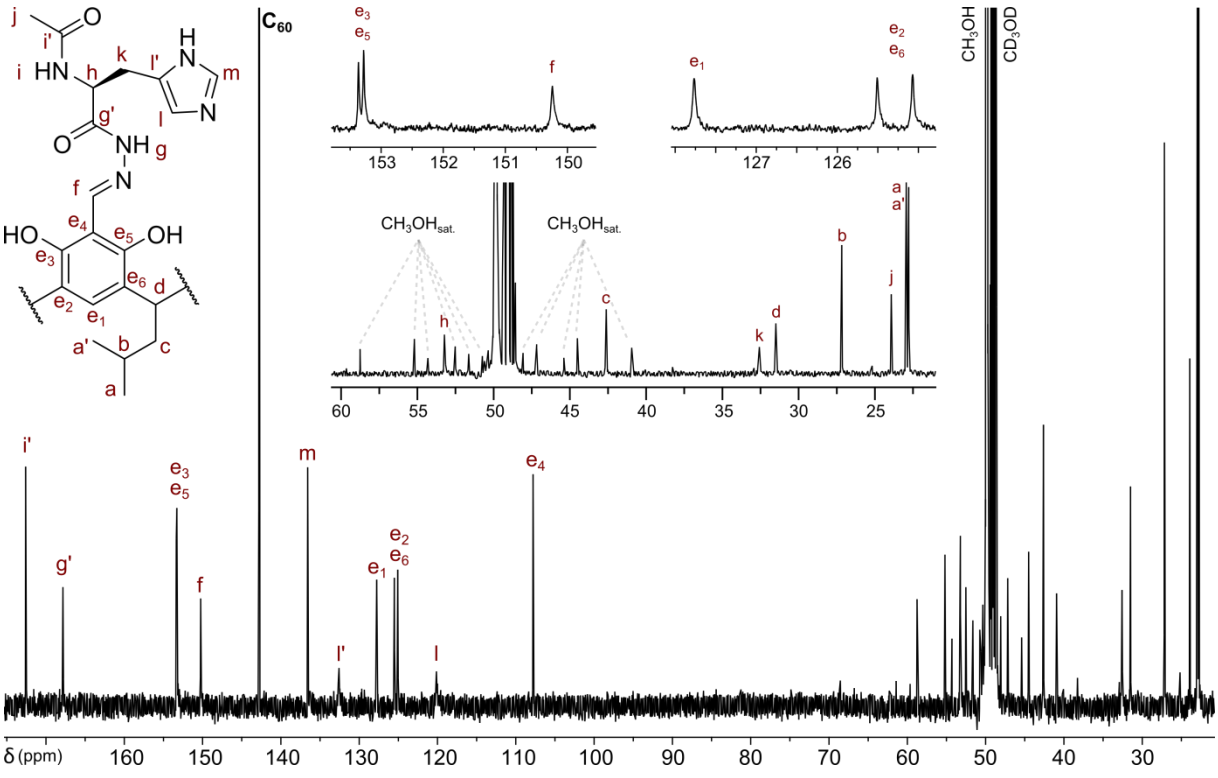

Fig. S41. ^{13}C NMR spectrum of (**3b**)$_2$⊃C_{60} (600 MHz, CD_3OD:CH_3OH, 1:9, *v*:*v*).

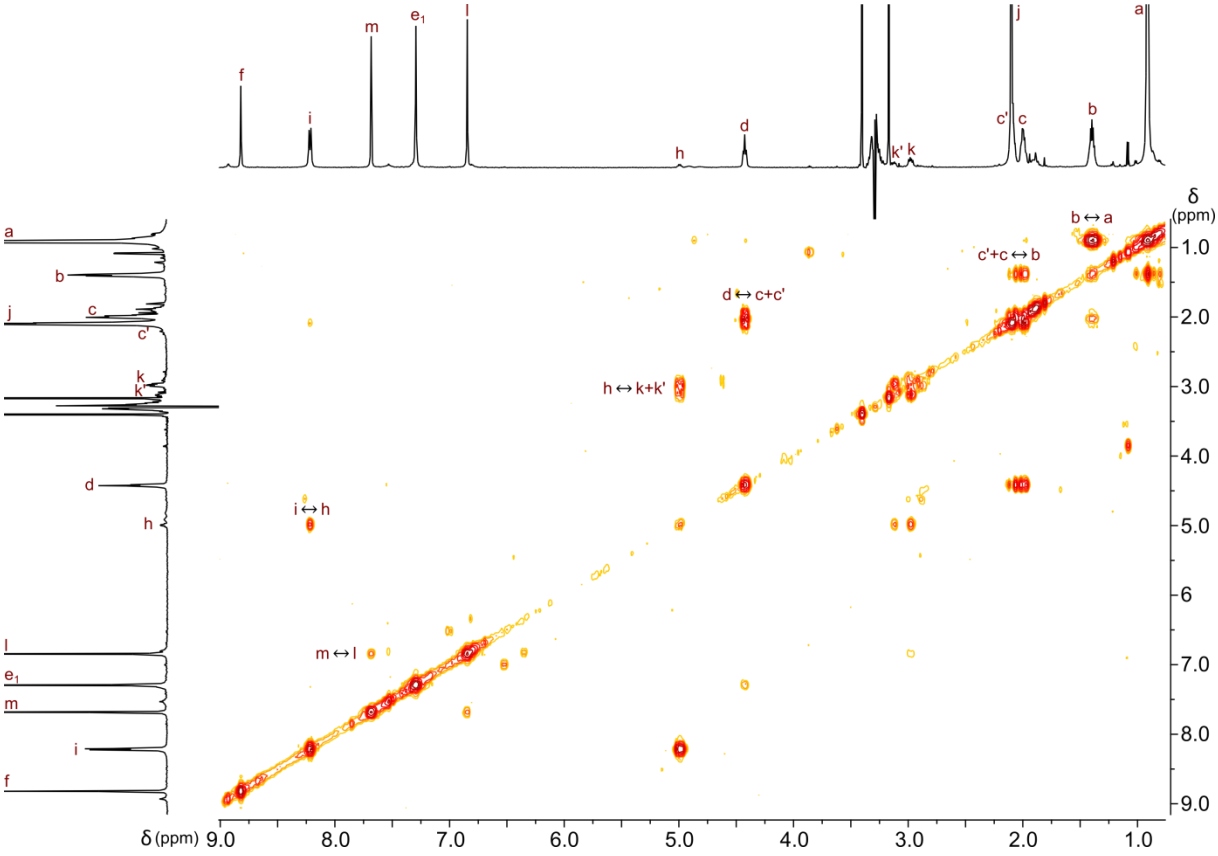

Fig. S42. ^{1}H-^{1}H COSY NMR spectrum of (**3b**)$_2$⊃C_{60} (600 MHz, CD_3OD:CH_3OH, 1:9, *v*:*v*).

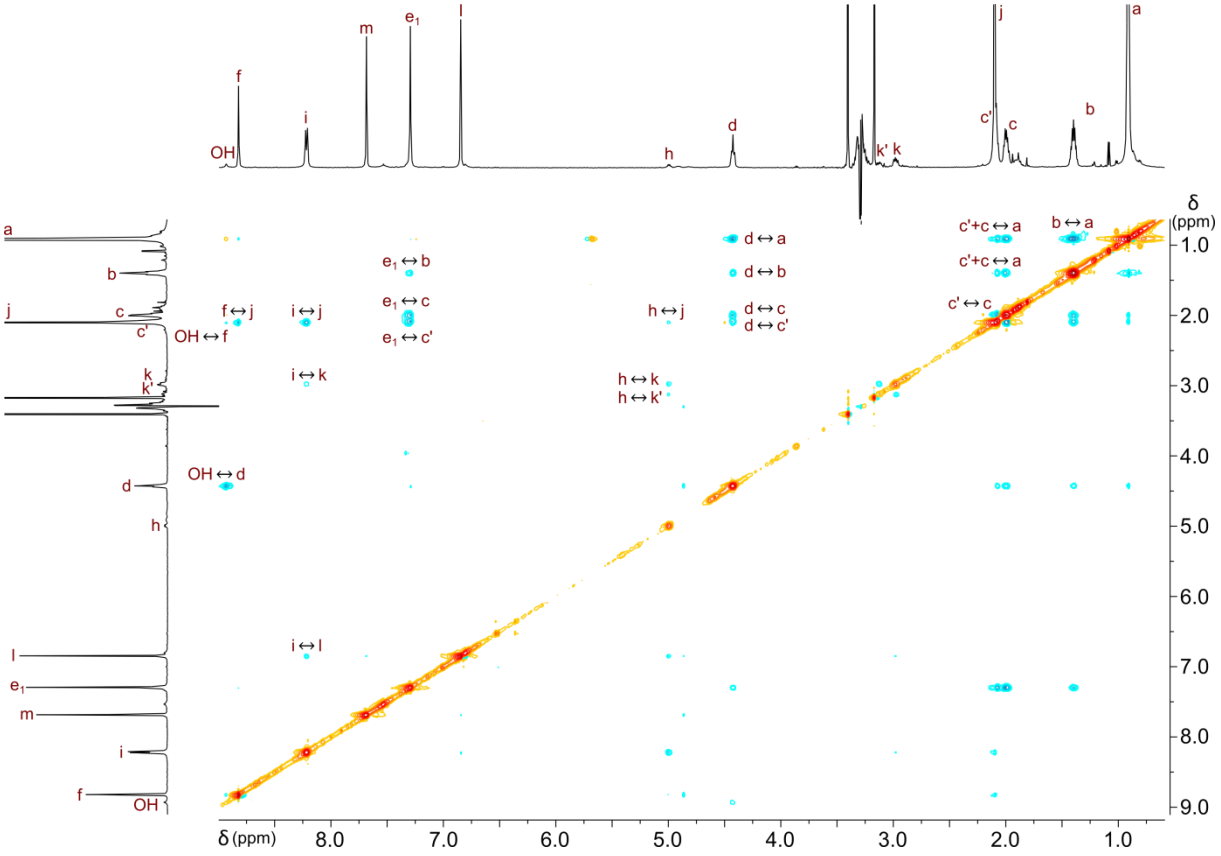

Fig. S43. ^{1}H-^{1}H ROESY NMR spectrum of (**3b**)$_2$⊃C_{60} (600 MHz, CD_3OD:CH_3OH, 1:9, *v*:*v*).

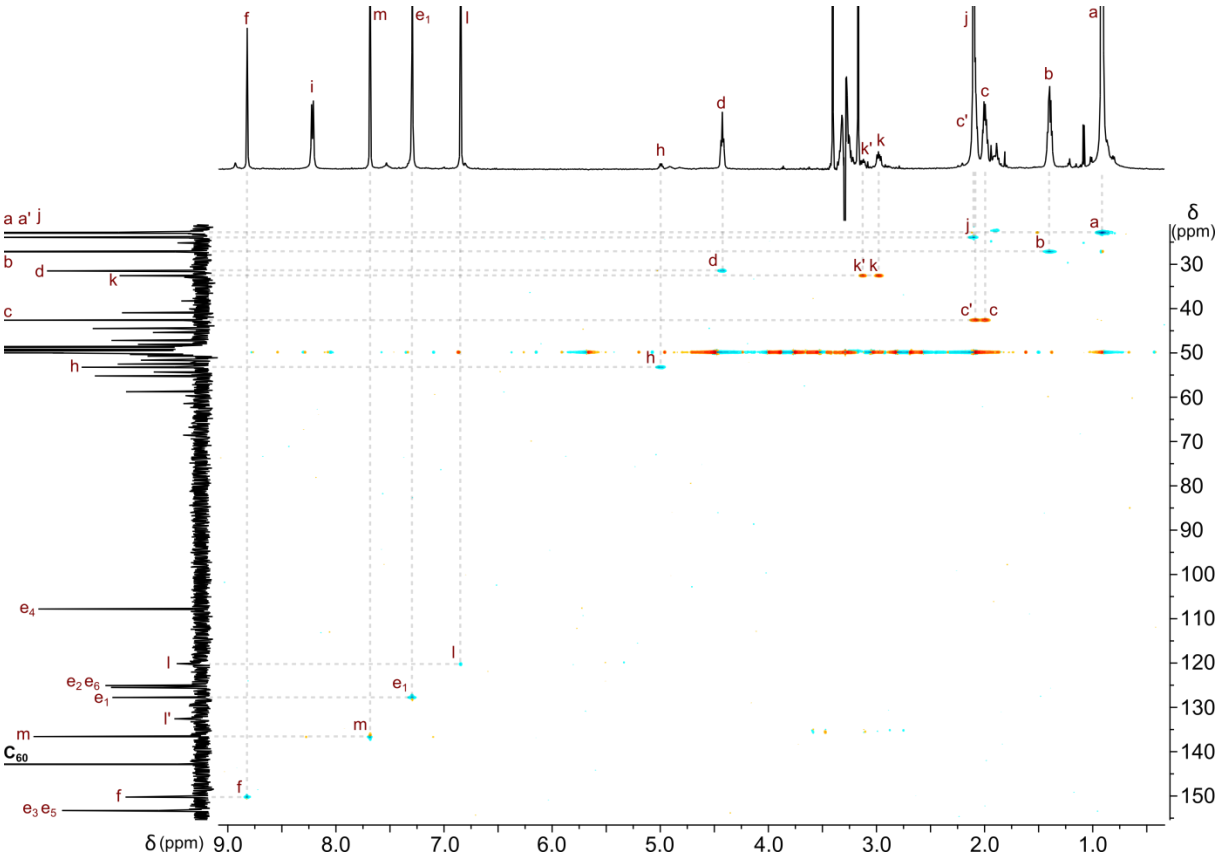

Fig. S44. ^{1}H-^{13}C HSQC NMR spectrum of (**3b**)$_2$⊃C_{60} (600 MHz, CD_3OD:CH_3OH, 1:9, *v*:*v*).

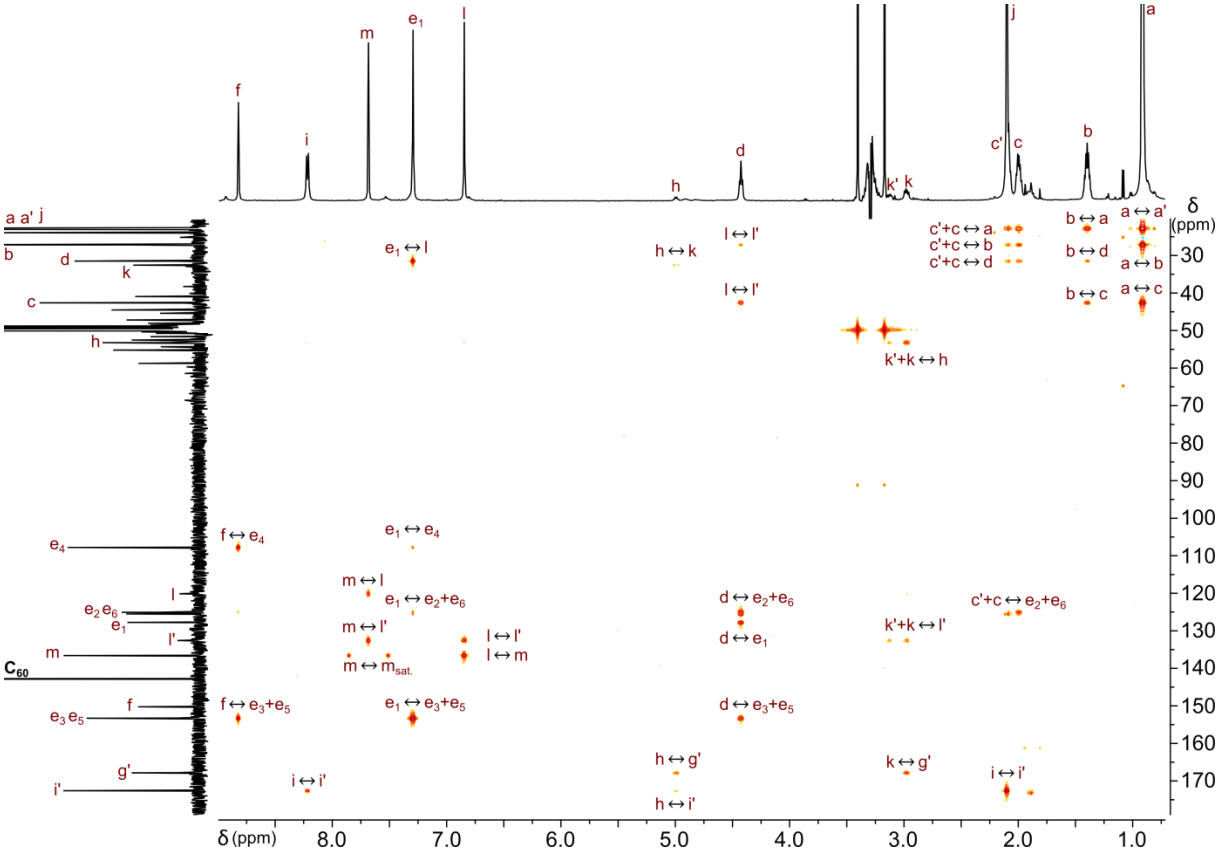

Fig. S45. ^{1}H-^{13}C HMBC NMR spectrum of (**3b**)$_2$⊃C_{60} (600 MHz, CD_3OD:CH_3OH, 1:9, *v*:*v*).

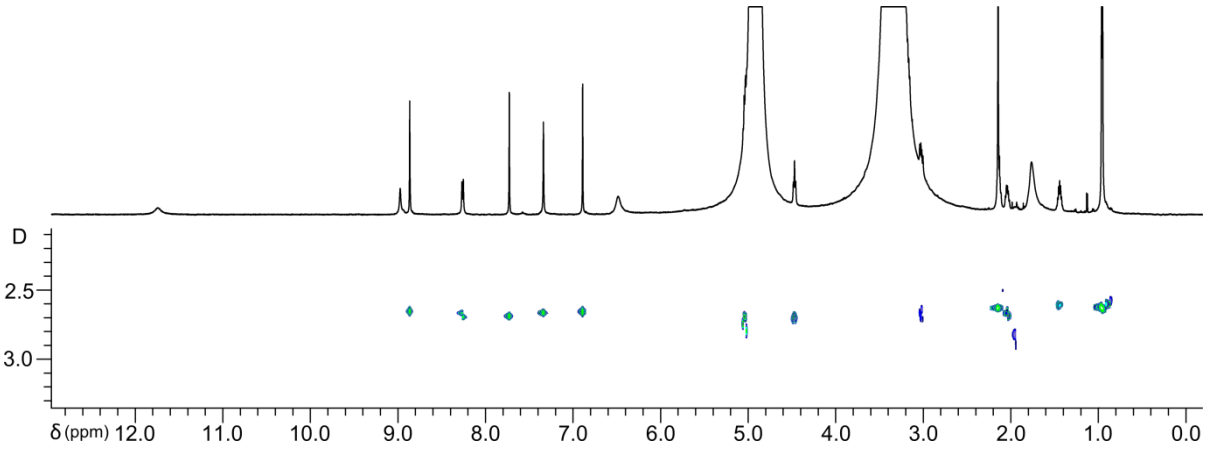

Fig. S46. DOSY NMR spectrum of (**3b**)$_2$⊃C_{60} (600 MHz, CD_3OD:CH_3OH, 1:9, *v*:*v*).

5.2. CD and UV-Vis spectra

a)

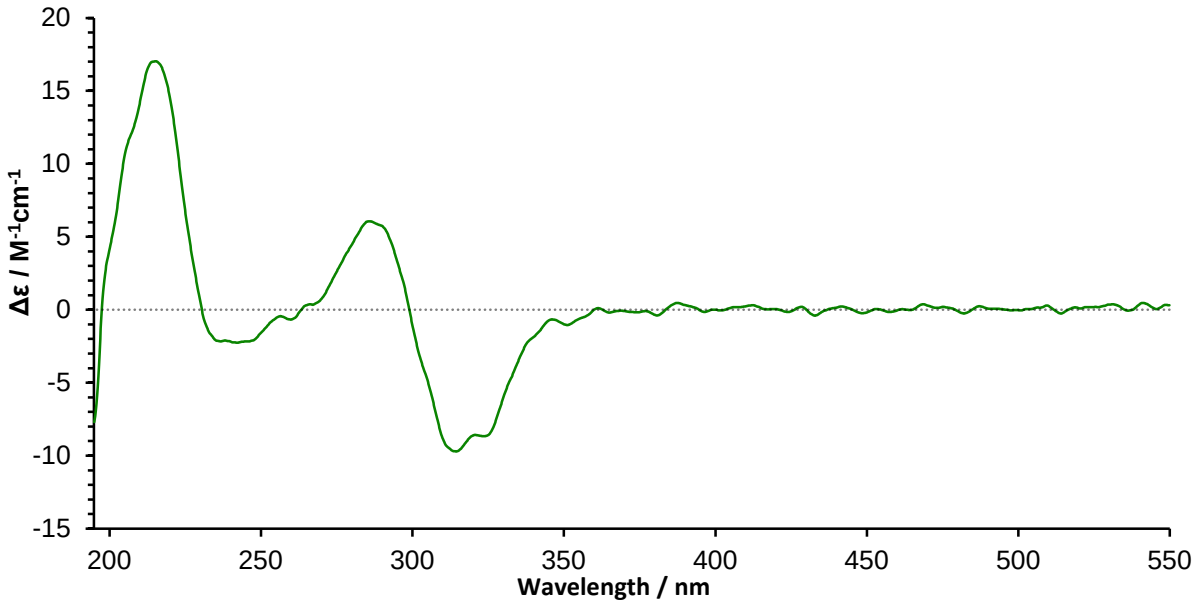

b)

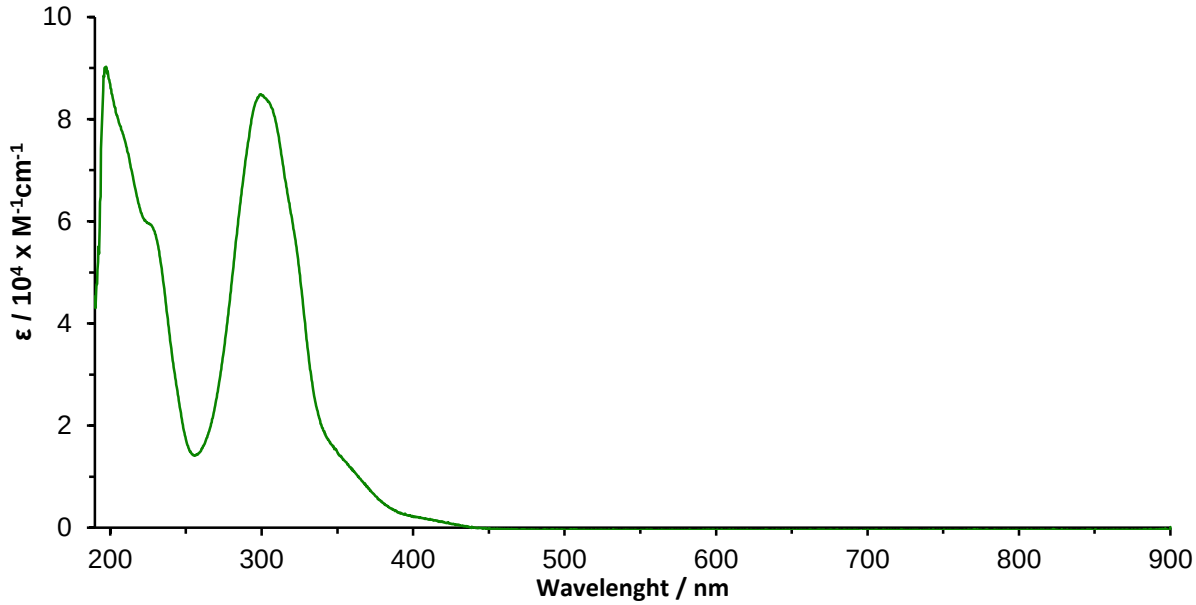

Fig. S47. a) ECD spectrum and **b)** UV-Vis spectrum of **3a** in MeOH (l = 0.2 cm, c = 0.0000401 mol/dm^3).

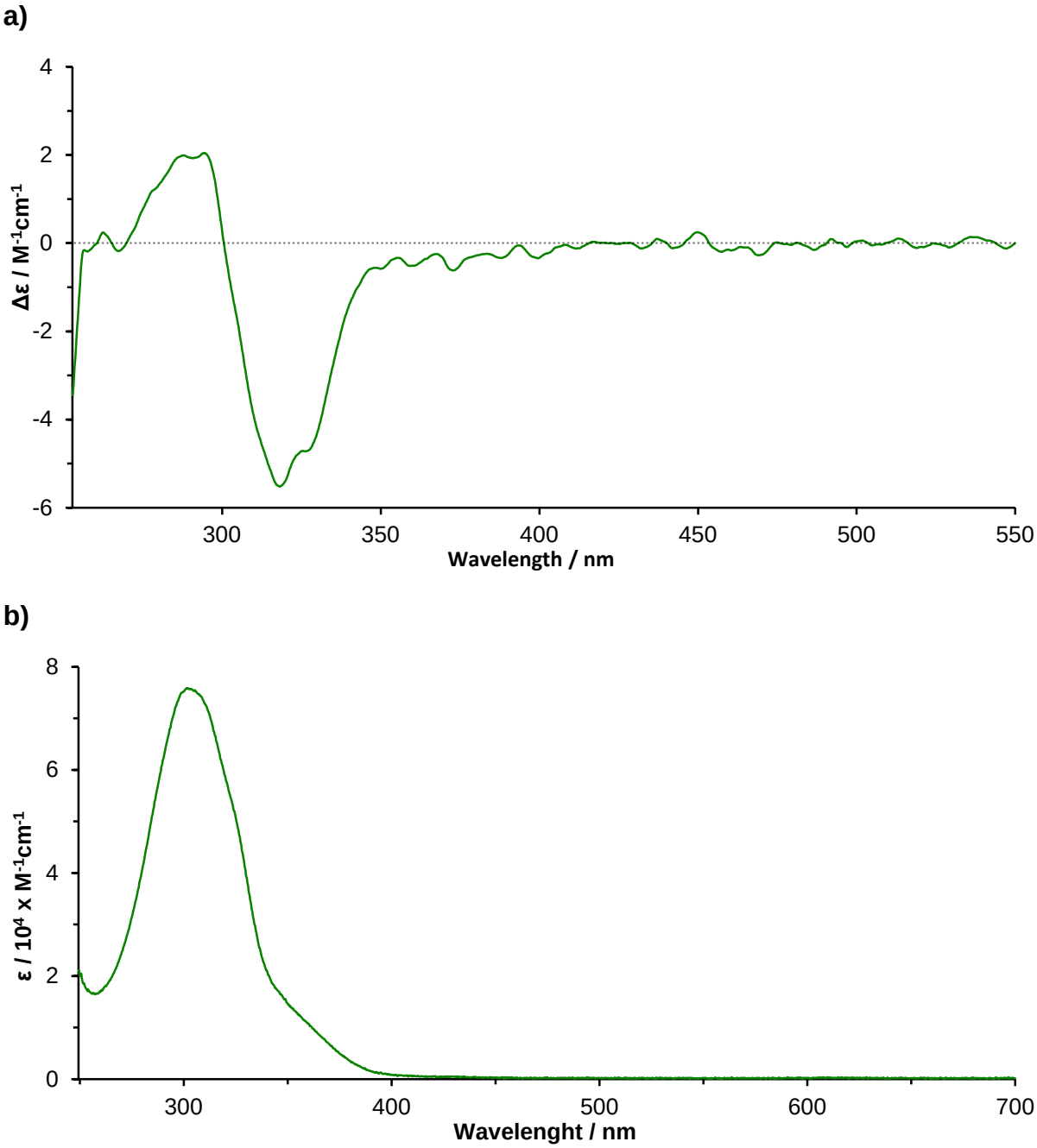

Fig. S48. a) ECD spectrum and **b)** UV-Vis spectrum of **3a** in DMSO.

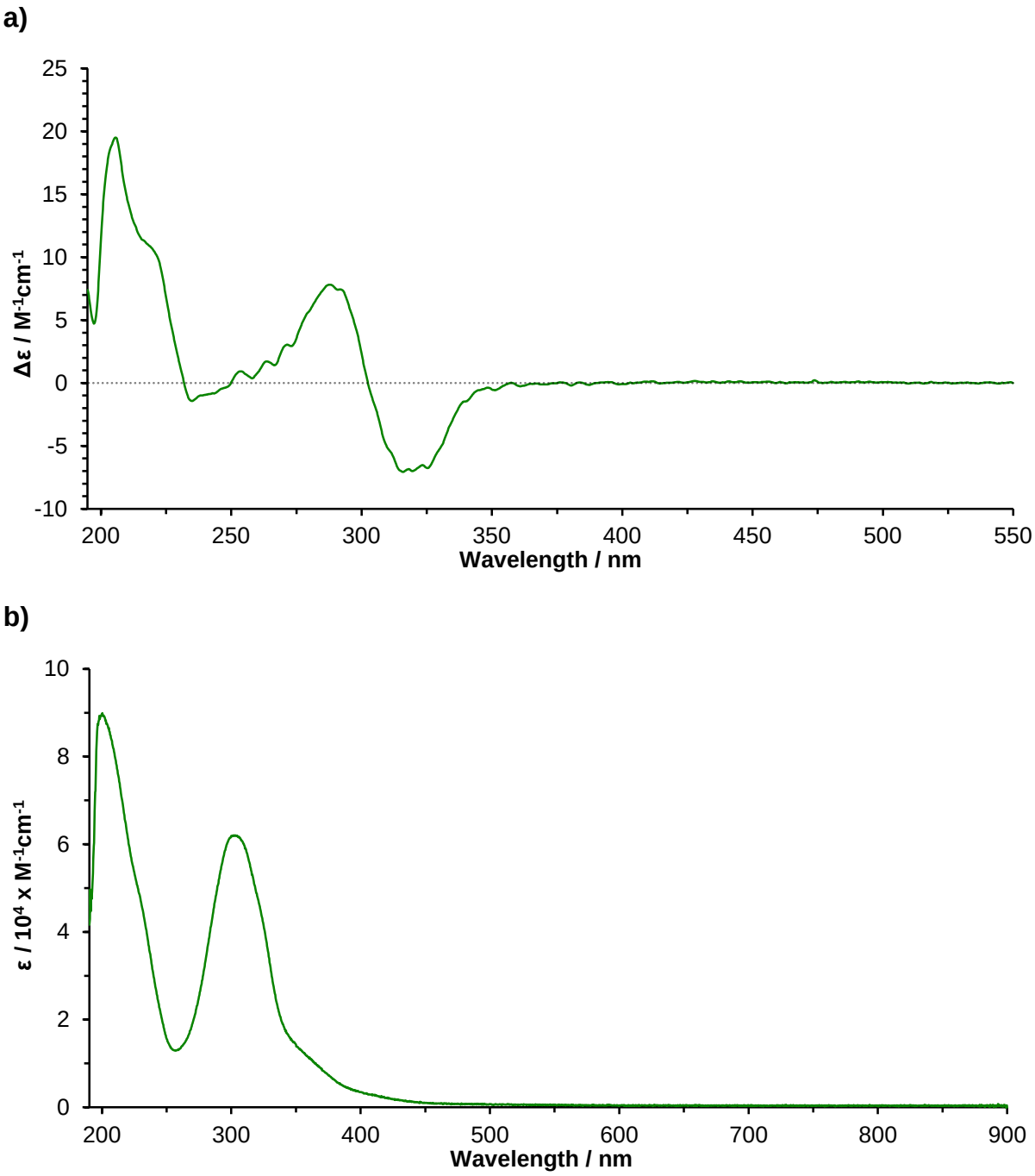

Fig. S49. a) ECD spectrum and **b)** UV-Vis spectrum of **3b** in MeOH.

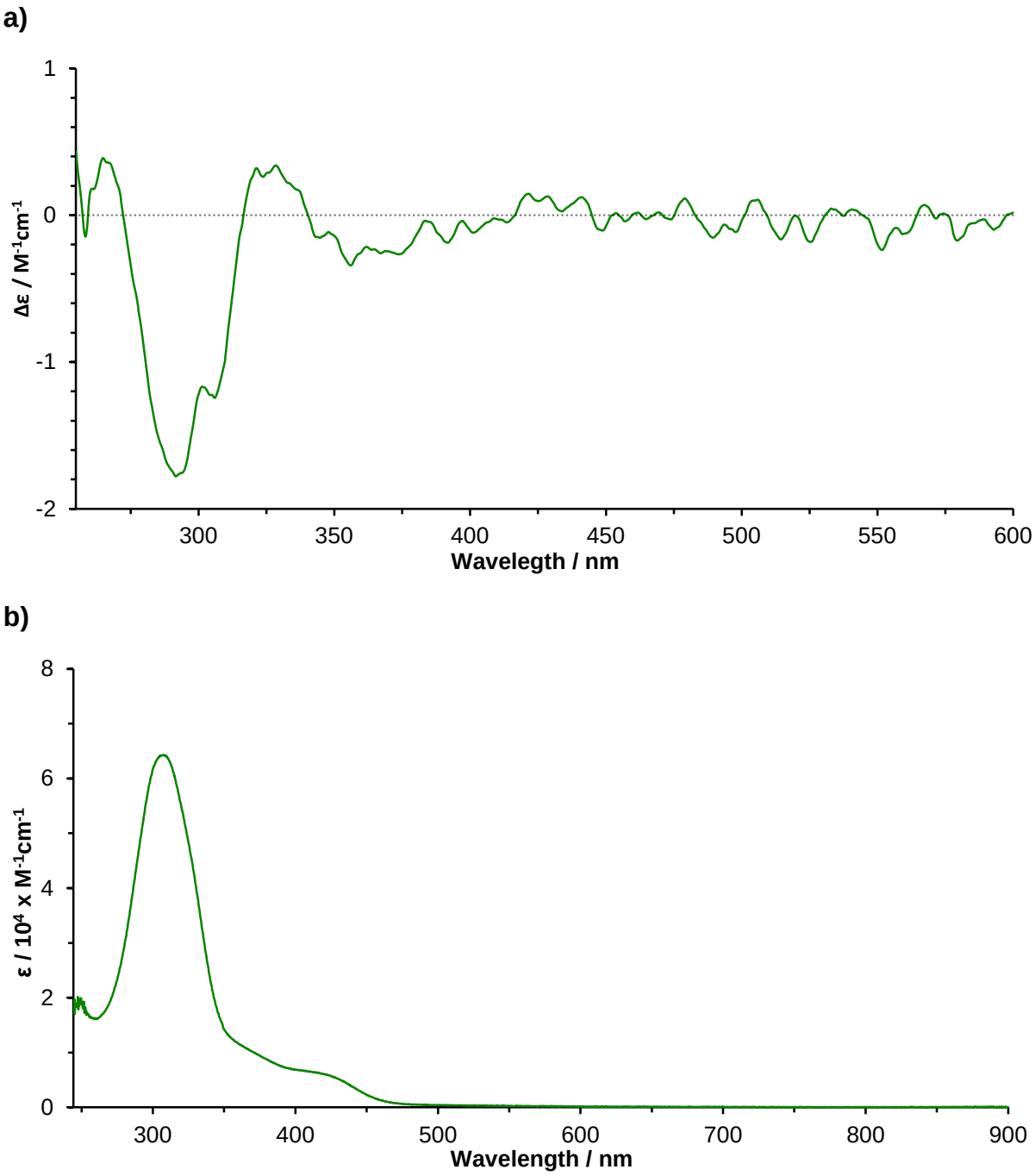

Fig. S50. a) ECD spectrum and **b)** UV-Vis spectrum of **3b** in DMSO.

a)

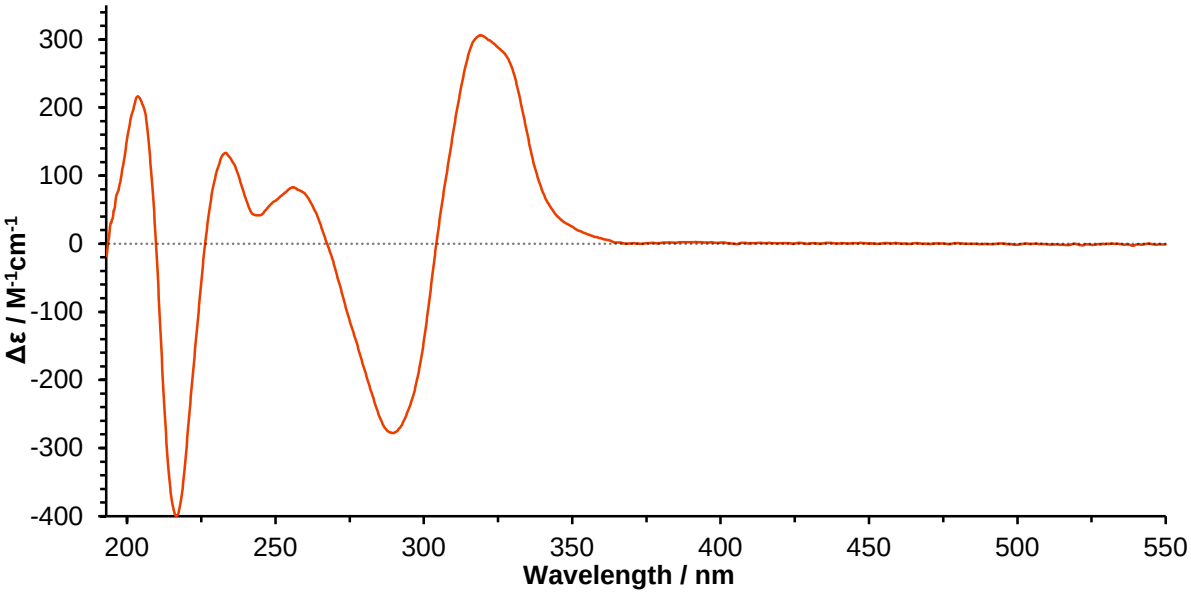

b)

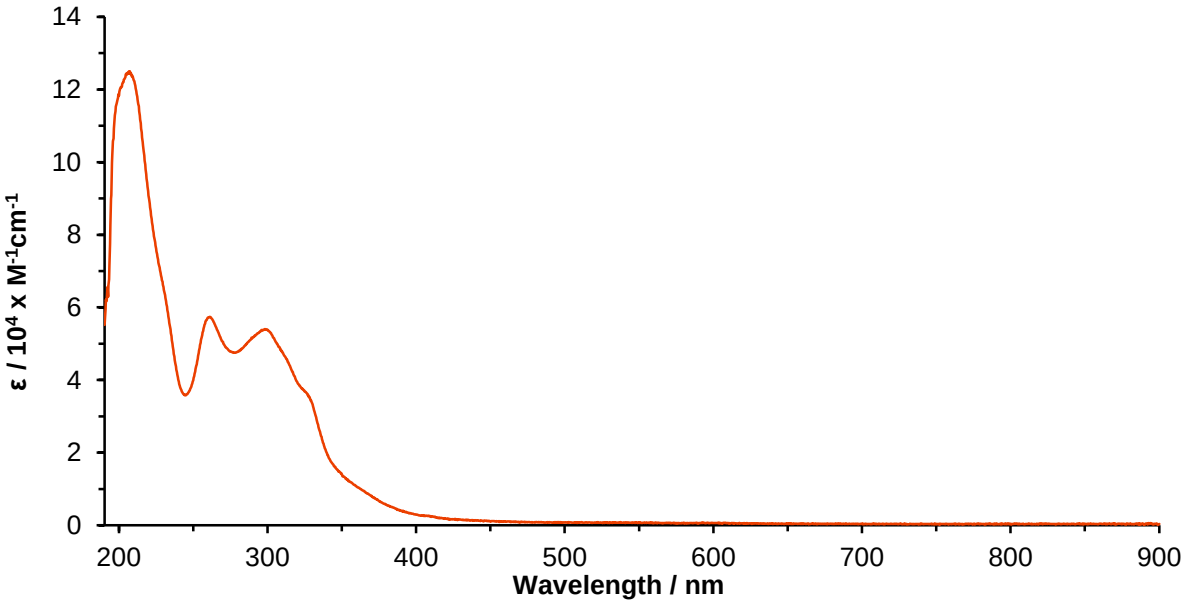

Fig. S51. a) ECD spectrum and **b)** UV-Vis spectrum of (**3b**)$_2$⊃C_{60} in MeOH.

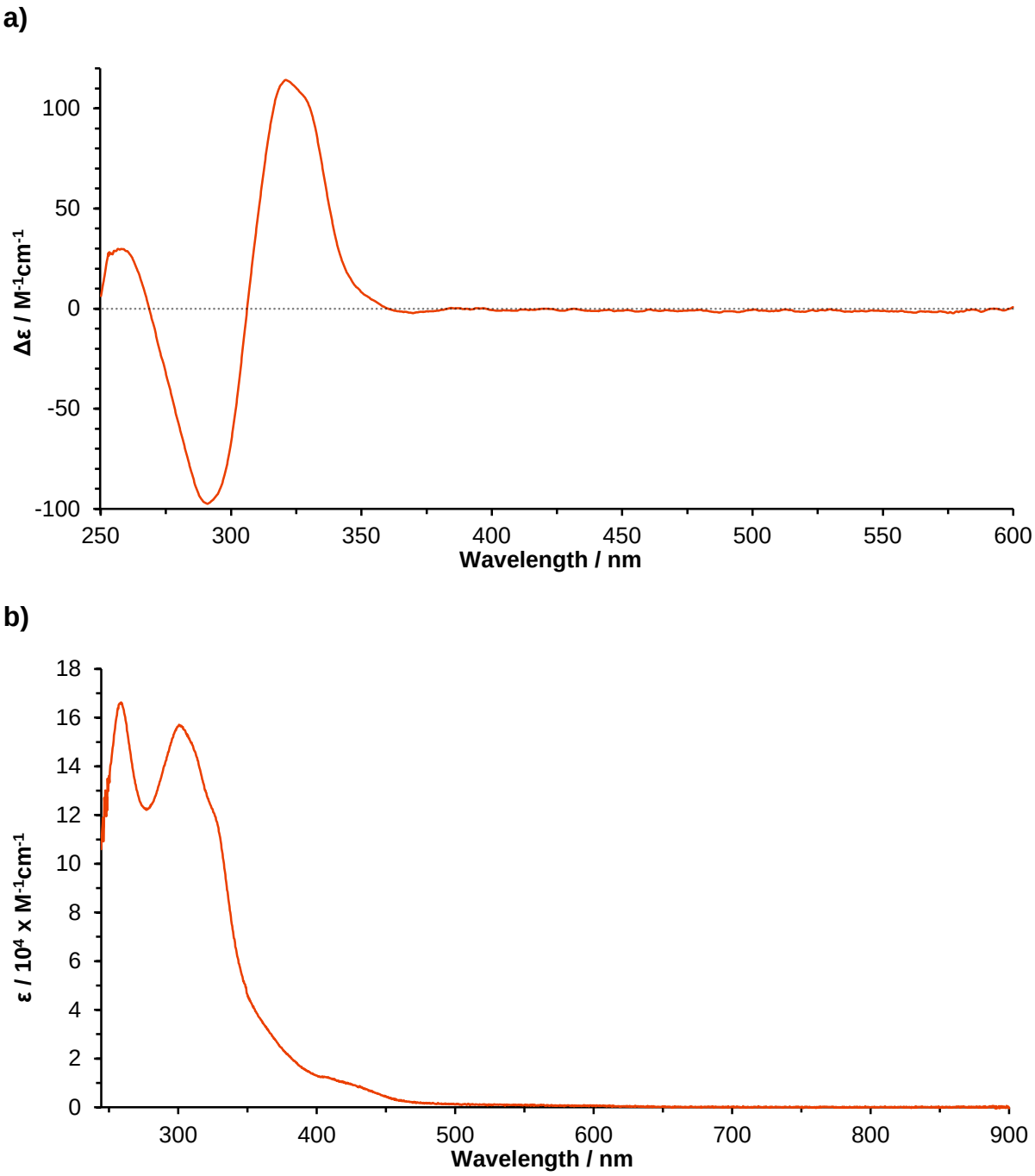

Fig. S52. a) ECD spectrum and **b)** UV-Vis spectrum of (**3b**)$_2$⊃C_{60} in DMSO.

5.3. MS spectra

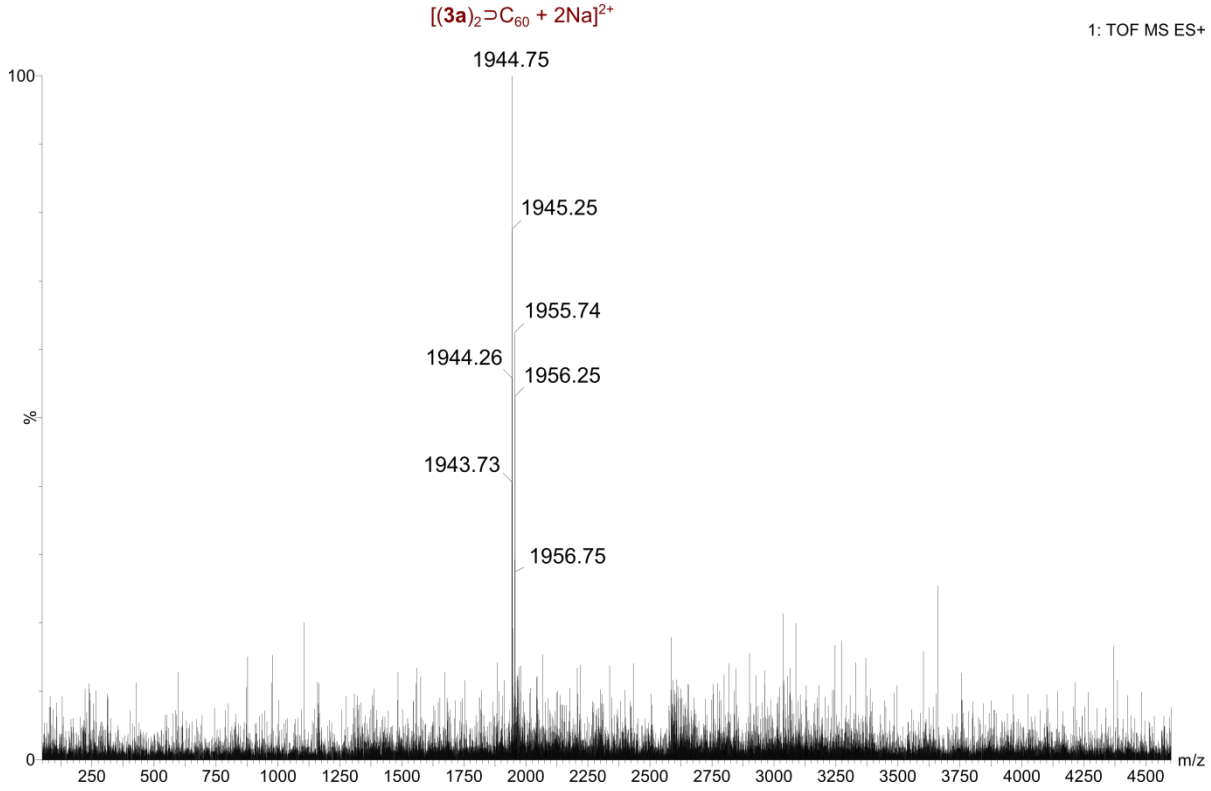

Fig. S53. TOF ESI MS spectrum of (**3a**)$_2$⊃C_{60}.

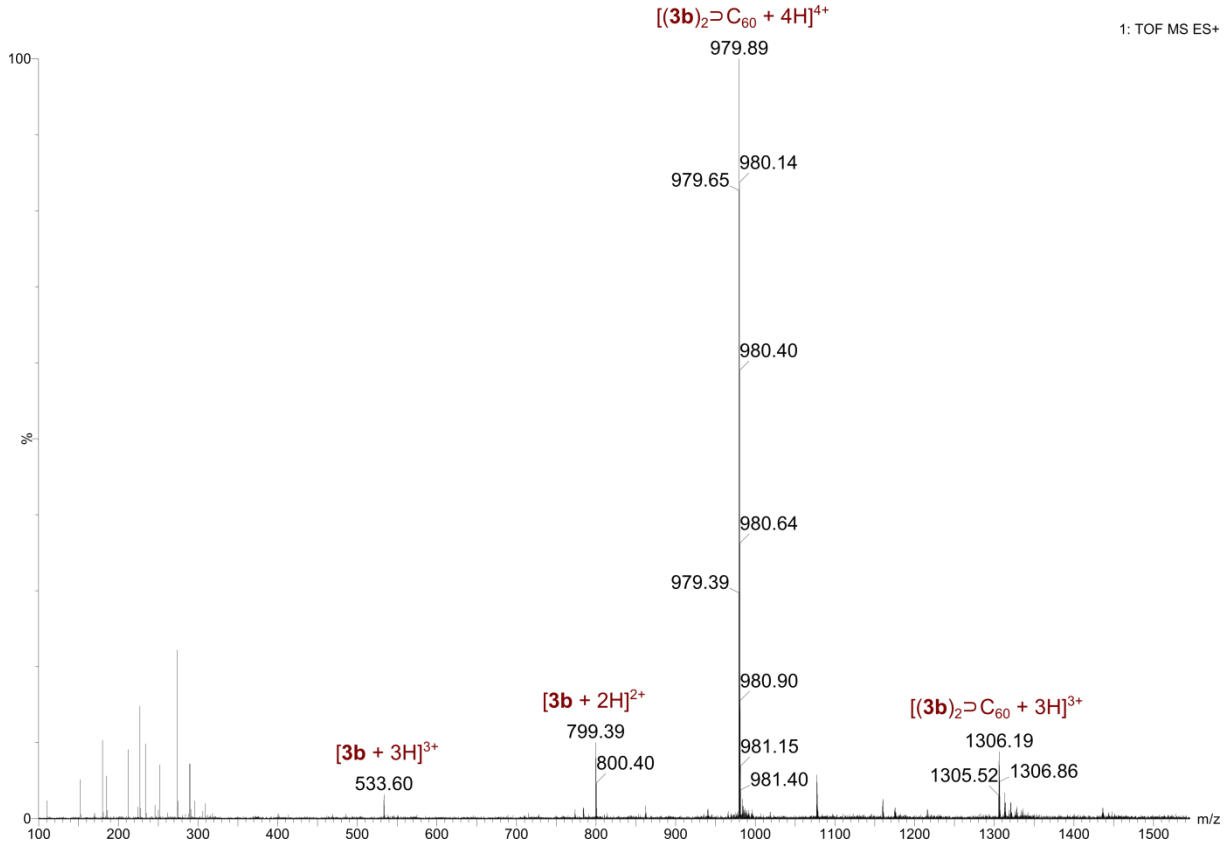

Fig. S54. TOF ESI MS spectrum of (**3b**)$_2$⊃C_{60}.